



**International Wigner Workshop**

**IWW 2021**

**Book of Abstracts**

**May 17-21, 2021**

**Virtual**

**[iww2021.sejong.ac.kr](http://iww2021.sejong.ac.kr)**

*hosted by the  
International Workshop on Computational Nanotechnology (IWCN) 2021*

**Edited by**

**Kyoung-Youm Kim  
Josef Weinbub  
Mark Everitt**

ISBN 978-3-9504738-2-7

© 2021 Institute for Microelectronics, TU Wien  
Gußhausstraße 27-29/E360, 1040 Wien, Austria

## Sponsored by



International Wigner Workshop  
[www.iww-meeting.info](http://www.iww-meeting.info)



Wigner Initiative  
[www.iue.tuwien.ac.at/wigner-wiki/](http://www.iue.tuwien.ac.at/wigner-wiki/)



Institute for Microelectronics, TU Wien  
[www.iue.tuwien.ac.at](http://www.iue.tuwien.ac.at)

Welcome to the **International Wigner Workshop (IWW) 2021**. Due to the COVID-19 pandemic, this instalment is organized as a live virtual event in the form of single sessions on the days of May 17-21. The workshop continues to bring together researchers from all areas of science and engineering areas in which Wigner functions have been or could be applied.

IWW 2021 marks the fourth instalment of the **International Wigner Workshop** series (see [www.iww-meeting.info](http://www.iww-meeting.info) for the full history) and further fosters the growing Wigner Initiative community ([www.iue.tuwien.ac.at/wigner-wiki/](http://www.iue.tuwien.ac.at/wigner-wiki/)). The speakers at this year's workshop provided an abstract which was reviewed by the program committee. Topics of interest related to the use of Wigner functions are (but not limited to): Computational or Numerical Challenges, Nanoelectronics, Nanostructures, Quantum Circuits, Quantum Information Processing, Quantum Optics, Quantum Physics, and Quantum Transport.

IWW 2021 hosts three invited and 32 regular speakers as well as 85 registered participants.

We would like to express our gratitude to our sponsors, our host workshop [IWCN 2021](#) and in particular its chair, Prof. Mincheol Shin (KAIST), as well as the participants who will make the workshop both interesting and successful. We hope that you enjoy it.

*Kyoung-Youm Kim, Josef Weinbub, and Mark Everitt*  
*Chairs of IWW 2021*  
*May, 2021*

### **General Chair**

**Kyoung-Youm Kim**, *Sejong University, Korea*

### **Co-Chair**

**Josef Weinbub**, *TU Wien, Austria*

### **Program Chair**

**Mark Everitt**, *Loughborough University, UK*

### **Program Committee**

**Wolfgang Belzig**, *University of Konstanz, Germany*

**David K. Ferry**, *Arizona State University, USA*

**Irena Knezevic**, *University of Wisconsin-Madison, USA*

**Mihail Nedjalkov**, *TU Wien, Austria and Bulgarian Academy of Sciences, Bulgaria*

**Franco Nori**, *RIKEN, Japan*

**Stefano Olivares**, *University of Milan, Italy*

**Xavier Oriols**, *Autonomous University of Barcelona, Spain*

**Siegfried Selberherr**, *TU Wien, Austria*

## Program

Time zone: UTC+2

Version: May 19, 2021

Monday, May 17

- 14:00    **Opening Remarks:** Kyoung-Youm Kim and Josef Weinbub
- 14:10    Todd Tilma [1](#)  
*Visualizations of Wigner Function Representations:  
The Discrete. The Continuous. And The “Weird”. (Invited)*
- 14:40    Oscar Dahlsten [2](#)  
*Tunnelling Necessitates Negative Wigner Function*
- 15:00    Ulysse Chabaud [4](#)  
*Witnessing Wigner Negativity*
- 15:20    Mustapha Ziane [6](#)  
*The Wigner Function Negativity and Non-Gaussian Entanglement*
- 15:40    Bartłomiej J. Spisak [8](#)  
*Dynamical Tunneling of the Defective Schrödinger Cat States*
- 16:00    Dariusz M. Woźniak [10](#)  
*Phase-Space Approach to Nonlinear Oscillator Under  
Periodic Electric Field*

Tuesday, May 18

- 14:00    Andrey Moskalenko [12](#)  
*Towards Quantum Tomography with Subcycle Temporal Resolution  
(Invited)*
- 14:30    Seongjin Ahn [14](#)  
*High-Order Harmonics Radiation and its Time-Frequency Wigner  
Representation for a Two-Level System Driven by Ultrashort Pulses*
- 14:50    Alexander Larkin [16](#)  
*Thermodynamic Properties of Unpolarized Uniform Electron Gas:  
Monte Carlo Simulations*

15:10	Benjamin Roussel	<a href="#">18</a>
	<i>A Time-Frequency Approach to Relativistic Correlations in Quantum Field Theory</i>	
15:30	Tom Rivlin	<a href="#">20</a>
	<i>Using Classical Wigner Dynamics to Elucidate Tunneling Times</i>	
15:50	Ben Lang	<a href="#">22</a>
	<i>Dissipative Phase Space Crystals in Josephson Circuits</i>	
16:10	Ci Lei	<a href="#">24</a>
	<i>Selective Correlations in Finite Quantum Systems: The Desargues and Pappus Properties</i>	

*Wednesday, May 19*

14:00	Zlatan Aksamija	<a href="#">26</a>
	<i>Thermoelectric Transport in Nanostructured Materials: The Wigner-Boltzmann Approach (Invited)</i>	
14:30	Marta Reboiro	<a href="#">28</a>
	<i>Exceptional Points from the Hamiltonian of a Hybrid Physical System</i>	
14:50	Michael te Vrugt	<a href="#">30</a>
	<i>Orientational Order Parameters for Arbitrary Quantum Systems</i>	
15:10	Thilo Hahn	<a href="#">32</a>
	<i>Wigner Function and Entropy Dynamics of a Single Phonon Mode Coupled to an Optically Excited Quantum Dot</i>	
15:30	Orazio Muscato	<a href="#">34</a>
	<i>Wigner Ensemble Monte Carlo Simulation Without Discretization Error of a GaAs Resonant Tunneling Diode</i>	
15:50	Luigi Barletti	<a href="#">36</a>
	<i>Quantum Transmission Conditions for the Simulation of Graphene Heterojunction Devices</i>	
16:10	Vito Dario Camiola	<a href="#">38</a>
	<i>Equilibrium Wigner Function for Fermions and Classical Particles</i>	

*Thursday, May 20*

- 14:00    Kyoung-Youm Kim [40](#)  
*Application of the Window Function to the Discrete Wigner Transport Equation to Overcome Its Momentum Resolution Limit*
- 14:20    Robert Kosik [42](#)  
*Open Boundary Conditions for the Wigner and the Characteristic von Neumann Equation*
- 14:40    Dirk Schulz [44](#)  
*Approximation of Multiband Hamiltonians for the Wigner Equation*
- 15:00    Makbule K. Eryilmaz [46](#)  
*On the Nonphysical Solutions to the Wigner Equation in Electronic Transport Simulation*
- 15:20    Matteo Villani [48](#)  
*On the Wigner-Boltzmann Equation of Motion for Scenarios with Non-Commuting Energy Momentum Operators*
- 15:40    Pascal Degiovanni [50](#)  
*Processing Quantum Signals Carried by Electrical Currents*
- 16:00    Vittorio Romano [52](#)  
*Quantum Corrected Hydrodynamical Models for Charge Transport Based on the Equilibrium Wigner Function*
- 16:20    Russell P. Rundle [54](#)  
*Quantum-State Verification in Phase Space*

*Friday, May 21*

- 14:00    Mustafa Amin [56](#)  
*Hybrid Quantum-Classical Mechanics: Lessons from Wigner*
- 14:20    Apostolos Vourdas [57](#)  
*Coherent Subspaces in a Hilbert Space with Prime Dimension and  $Q$  Functions*

14:40	Emanuele Poli	<a href="#">58</a>
	<i>Wigner-Function Applications in Magnetic-Confinement Fusion: Propagation of High-Frequency Beams and Evolution of Geodesic- Acoustic Packets</i>	
15:00	Giovanni Manfredi	<a href="#">60</a>
	<i>Wigner Dynamics with Spin Effects</i>	
15:20	Alfredo M. Ozorio de Almeida	<a href="#">61</a>
	<i>Distinguishing Quantum Features in Classical Propagation</i>	
15:40	Hannes Weber	<a href="#">62</a>
	<i>Wigner-Function-Based Solution Schemes for Electromagnetic Wave Beams in Fluctuating Media</i>	
16:00	Mauro Ballicchia	<a href="#">64</a>
	<i>Modeling Coulomb Interaction with a 'Wigner-Poisson' Coupling Scheme</i>	
16:20	<b>Closing Remarks</b>	



# Visualizations of Wigner Function Representations: The Discrete. The Continuous. And The “Weird”.

Todd Tilma

*Tokyo Institute of Technology, Japan*

*Loughborough University, UK*

*todd.tilma@tilma-labs.org*

The rise of computer graphics and personal computers in the last half-century has allowed the visualization of multi-dimensional mathematical structures to become almost a field unto itself. Phase space functions, in particular the Wigner function, have a unique place in said visualizations; we need to look no further than the 2012 Nobel Prize in Physics, awarded in part to Serge Haroche for his experimental work that resulted in the complete reconstruction of a Schrodinger cat state Wigner function (the visualizations in the 2008 Nature paper [1] - is what “sealed the deal” in many minds).

In the last few years we have seen real-time Wigner function reconstructions and visualizations being available on the IBM quantum machine; multiple papers showcasing applets and codes to visualize the Wigner function for multi-particle quantum states; and the rise of augmented reality software that allows researchers to “fly thru” slices of a multi-dimensional Wigner function. In short, the future of phase space mathematics is bright and seems to be, in this researcher’s opinion, in the development of mathematical formulations that allow for the efficient and informationally complete reconstruction and visualization of multi-particle quasi-probability functions; showing as many dimensions as possible without having to incur informational or conceptual loss.

In this talk I will review the current and possible future state of Wigner function visualization; focusing on the discrete, the continuous, and the “weird” cases that comprise our field.

[1] S. Deléglise *et al.*, Nature 455, 510 (2008)

# Tunnelling Necessitates Negative Wigner Function

Yin Lin Long<sup>1</sup> and Oscar Dahlsten<sup>2</sup>

<sup>1</sup>*Blackett Laboratory, Imperial College London, London, United Kingdom, SW7 2BB*

<sup>2</sup>*Institute for Quantum Science and Engineering, Department of Physics, Southern University of Science and Technology (SUSTech), Shenzhen, attn.lin@gmail.com;dahlsten@sustech.edu.cn*

Quantum objects can ‘tunnel’ into and through barriers. Whilst it appears well-accepted that tunnelling contrasts with classical mechanics, being a wave-like behaviour exhibited by particles, from a quantum information science viewpoint one may wonder whether it is also non-classical in a probability theory sense. For example, in the context of adiabatic quantum computing and annealing it is conjectured that tunnelling plays a role in achieving quantum speed-up in computations. For this to be case, we expect that tunnelling should involve non-classical probabilistic behaviour, so that this process is non-classical at the level of data and probabilities. In fact, there are intriguing examples connecting tunnelling with *negativity* in the quasi-probability Wigner function representation of the quantum state. We therefore here aim to clarify the relation between negative Wigner function and tunnelling.

We give a clear mathematical definition of tunnelling which allows us to clarify this relation. We prove mathematically that a non-zero tunnelling rate necessitates a negative Wigner function. More specifically, the Wigner function of the state and/or the tunnelling rate operator have to contain negative values at some phase space points, see Fig.1. We thus make it concrete how tunnelling is associated with negative Wigner function, a prototypical non-classical probabilistic behaviour. We show how to apply the main theorem to several examples, including explaining how positive Wigner function states can tunnel due to negativities in an operator associated with the energy.

To investigate the phenomenon more deeply we also consider whether post-quantum theories could have a higher tunneling rate than quantum theory. We pose that as an open question and contribute tools for tackling it, by showing that the Wigner function, as a real-vector representation of quantum states, fits into the generalised probabilistic framework, thus allowing for a natural extension to post-quantum theories.

[1] Y. L. Long, O. Dahlsten, Phys. Rev. A 102, 062210 (2020)

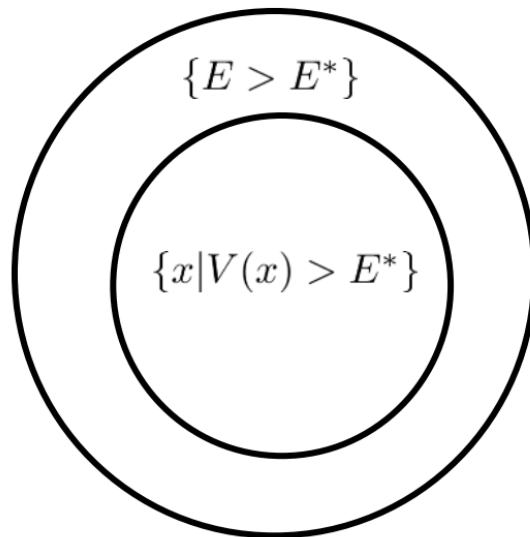


*Fig. 1: Why negative quasi-probability is needed for tunnelling. The phase space points where the potential energy  $V(x) > E^*$ , for some given energy  $E^*$  are a subset of the points for which the energy  $E > E^*$ . Thus, for classical probability theory we have an inequality between the associated probabilities:  $P(x|V(x) > E^*) \leq P(E > E^*)$ . We define quantum tunnelling as violation of this inequality. In the quantum phase space the Wigner function replaces the classical probability density, and the former can be negative, which makes violation of the inequality possible.*

# Witnessing Wigner Negativity

Ulysse Chabaud<sup>1,2</sup>, Pierre-Emmanuel Emeriau<sup>3</sup>, and Frédéric Grosshans<sup>3</sup>

<sup>1</sup>*Department of Computing and Mathematical Sciences, California Institute of Technology*

<sup>2</sup>*Université de Paris, IRIF, CNRS, France*

<sup>3</sup>*Sorbonne Université, CNRS, LIP6, F-75005 Paris, France*

*pierre-emmanuel.emeriau@lip6.fr*

Negativity of the Wigner function is arguably one of the most striking non-classical features of quantum states [1]. Beyond its fundamental relevance, it is also a necessary resource for quantum speedup with continuous variables [2,3]. As quantum technologies emerge, the need to identify and characterize the resources which provide an advantage over existing classical technologies becomes more pressing [4].

In our work, we derive a complete family of experimentally accessible witnesses for Wigner negativity of quantum states, based on fidelities with Fock states. Witnesses are observables that possess a threshold expected value indicating whether the measured state exhibits the desired property or not (see Fig. 1). Our witnesses can be reliably measured using photo-number detector as well as homodyne or heterodyne detection [7].

For our Wigner negativity witnesses, we phrase the problem of finding the threshold value as an infinite-dimensional linear optimisation. By relaxing and restricting the corresponding linear programs, we derive two hierarchies of semidefinite programs which allow us to obtain numerical sequences of upper and lower bounds for the threshold values (see Fig. 2). Additionally, we show that both of these sequences converge to the threshold value, by employing tools from infinite-dimensional optimization theory [5,6]. This provides a reliable method for detecting Wigner negativity of quantum states (see Fig. 3).

Our work is thought to be interesting for physicists interested in characterizing Wigner negativity of quantum states—either theoretically or experimentally—and mathematicians interested in infinite-dimensional convex optimisation theory.

*Editorial note: This abstract is based on [8].*

[1] E. P. Wigner, In Part I: Physical Chemistry. Part II: Solid State Physics, p.110-120

(Springer, 1997)

[2] S. Lloyd, S. L. Braunstein, In Quantum Information with Continuous Variables, p.9-17

(Springer, 1999)

[3] A. Mari, J. Eisert, Phys. Rev. Lett. 109, 230503 (2012)

[4] J. Preskill, Quantum 2, 79 (2018)

[5] J. B. Lasserre, SIAM J. Optimiz. 11(3), 796–817 (2001)

[6] P. A. Parrilo, PhD thesis (California Institute of Technology, 2000)

[7] U. Chabaud *et al.*, arXiv:2011.04320 (2020)

[8] U. Chabaud *et al.*, arXiv:2102.06193 (2021)

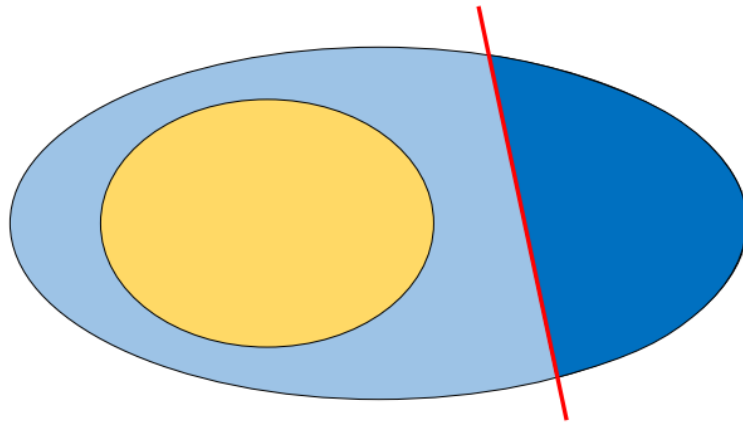


Fig.1: Pictorial representation of a witness. In yellow: states without the property. In blue: states with the property. In red: witness threshold value. In light blue, states undetected by the witness. A complete family of witnesses for a given property is a set of witnesses such that each state having the property is detected by at least one witness from the family.

N	Lower bound	Upper bound
1	0.5	0.5 (0.528)
2	0.5	0.5 (0.551)
3	0.378	0.427
4	0.375	0.441
5	0.314	0.385
6	0.314	0.378
7	0.277	0.344
8	0.280	0.348
9	0.256	0.341
10	0.262	0.334

Fig.2: Table of numerical upper and lower bounds for the threshold value of various witnesses obtained using our hierarchies of semidefinite programs. The Wigner negativity witnesses considered here are fidelities with Fock states (photon-number states  $|N\rangle$ ) from 1 to 10. The bounds in the first two lines are analytical (numerical values between parentheses). For example, having a state  $\rho$  such that  $\langle 7|\rho|7\rangle > F_7$  guarantees that  $\rho$  shows Wigner negativity, and  $0.277 \leq F_7 \leq 0.344$ . Furthermore, for any  $F < F_7$ , there exist a state  $\sigma$  with a positive Wigner function, such that  $\langle 7|\sigma|7\rangle = F$ .

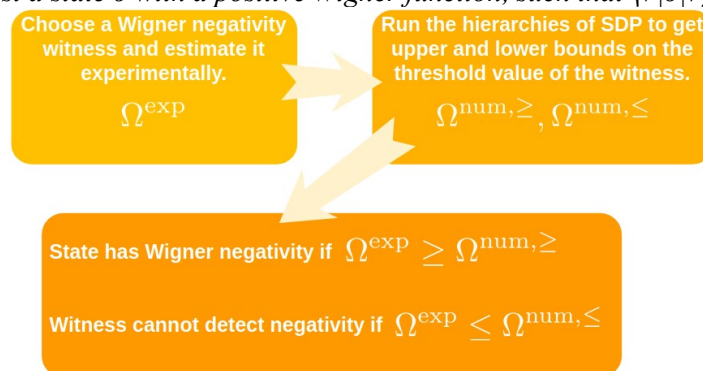


Fig.3: Protocol for witnessing Wigner negativity using our witnesses.

# The Wigner Function Negativity and Non-Gaussian Entanglement

Mustapha Ziane and Morad El Baz

*Mohammed V university, Faculty of sciences, Rabat, Morocco*

*mustapha\_ziane@um5.ac.ma*

In the field of quantum information science, quantum correlations are an essential tool for improving several protocols in quantum information-processing compared to their classical analogs. In this direction, the search for adequate measures of these correlations is of paramount importance. In particular, entanglement quantifying is one of the priority problems of quantum information theory. On the other hand, continuous-variable systems with non-Gaussian entangled states are known to have more entanglement amount. Hence, non-Gaussian systems are better resources for quantum information processing protocols, such as quantum teleportation.

In this thesis, we address the issue of entanglement identifying in discrete and continuous variables systems providing a new approach to quantify the entanglement in continuous-variable states. We introduce and develop a geometric measure of entanglement for the class of non-Gaussian states based on the negativity property of the Wigner function. We prove that this quantity satisfies the natural properties expected from a good entanglement monotone.

We evaluate and analyze this entanglement measure for some relevant bipartite systems, and investigate the relevance of this approach to visualize and quantify the different kinds of entanglement in the case of multipartite systems. We show qualitatively that our quantity can serve as a direct measure of genuine entanglement in tripartite states, independently of bipartite constructions.

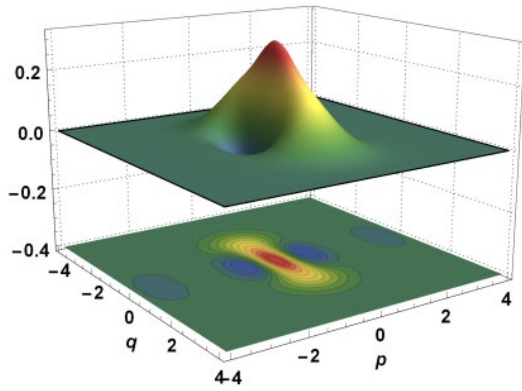


Fig.1: The Wigner function of Schrödinger cat state with odd coherent states

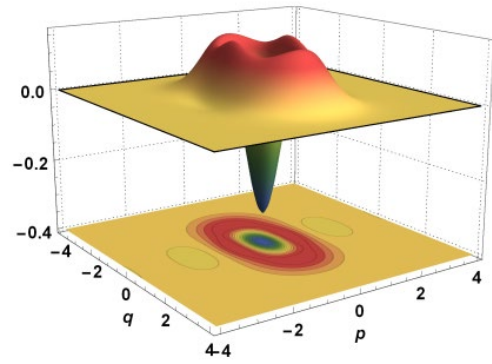


Fig.2: The Wigner function of Schrödinger cat state with with even coherent states.

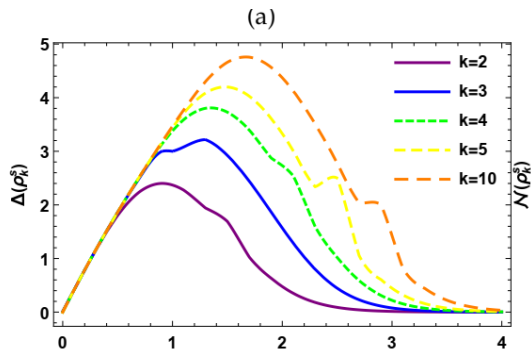


Fig.2: Change in our quantity versus the squeezing parameter for two mode quasi vortex state.

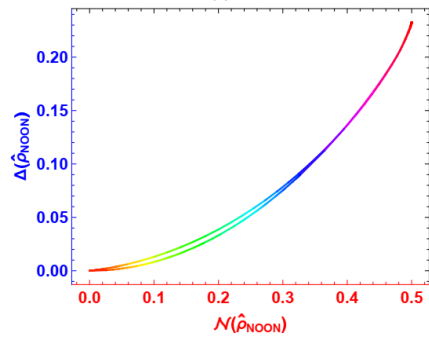


Fig.5 Parametric plot of our quantity versus the entanglement for fixed values of the photon number in NOON states.

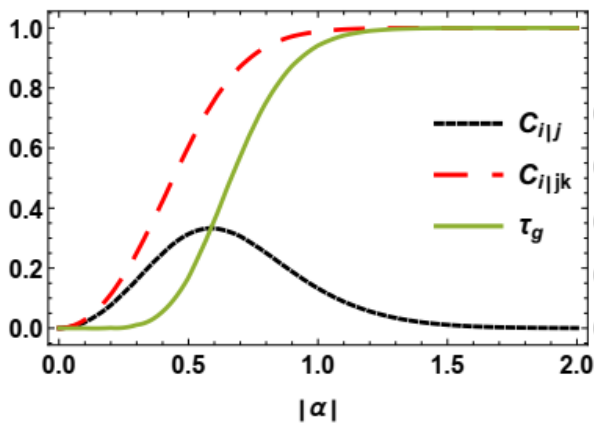


Fig.3: The behavior of different kinds of entanglement in tripartite GHZ class of coherent states

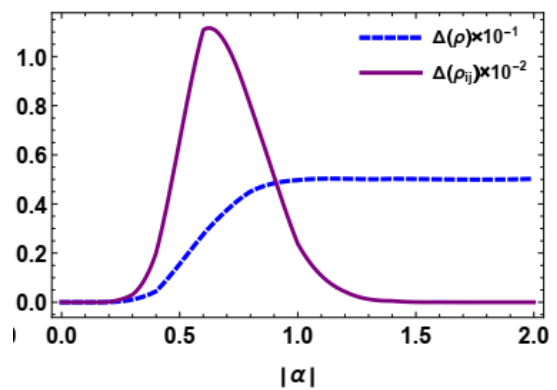


Fig.6: Our quantity versus the field amplitude for GHZ tripartite class of coherent states

# Dynamical Tunneling of the Defective Schrödinger Cat States

Bartłomiej J. Spisak, Damian Kołaczek, and Maciej Wołoszyn

*AGH University of Science and Technology*

*Faculty of Physics and Applied Computer Science*

*bjs@agh.edu.pl*

The concept of tunneling is one of the central issues of quantum physics. Description of this phenomenon is usually based on the transmission coefficient which is calculated by means of the plane waves. This approach, however, becomes unpractical when the electron state cannot be characterized in this way [1]. Hence, a natural question arises, how to calculate the transmission coefficient for states represented by others types of wavefunctions? This general question defines the problem being a subject of the presented contribution.

By applying the phase-space description [2,3] we investigate a problem of the dynamical tunneling [4] of a defective superposition of two well separated Gaussian wavepackets through the dispersive medium containing a repulsive obstacle. This non-classical state is called the defective Schrödinger cat state. For this purpose, we construct the Wigner distribution functions for the family of these defective non-classical states, and we determine the influence of this defectiveness on the Wigner distribution function dynamics by solving its equation of motion in the Moyal form [5]. We pay special attention to the dynamical quantumness of this state and its localization in the above-barrier reflection regime [6,7].

[1] E. Merzbacher., *Phys. Today* 55, 44 (2002)

[2] E. P. Wigner, *Phys. Rev.* 40, 749 (1932)

[3] J. E. Moyal, *Proc. Camb. Phil. Soc.* 45, 99 (1949)

[4] E. Heller, *J. Chem. Phys. A* 103, 49 (1999)

[5] D. Kołaczek *et al.*, *Int J. Appl. Math. Comput. Sci.* 29, 439, (2019)

[6] A. Kenfack, K. Życzkowski, *J. Opt. B: Quantum Semiclass. Opt.* 6, 396 (2004)

[7] P. Garbaczewski, *Entropy* 7, 253 (2005)

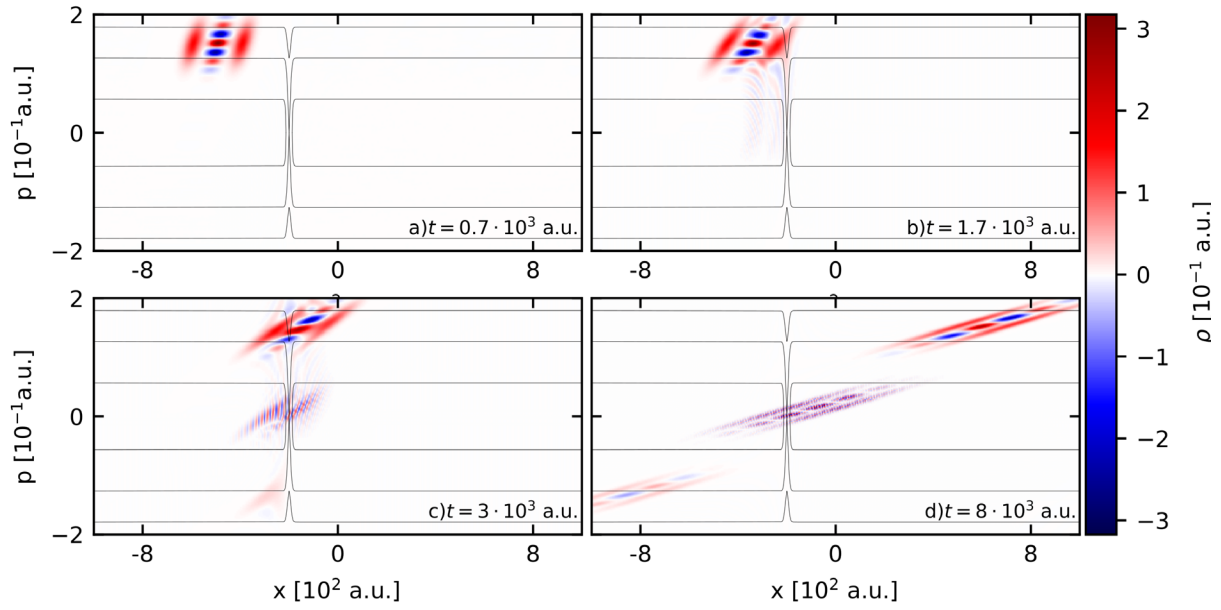


*Fig. 1: Dynamics of the Wigner distribution function representing a defective Schrödinger cat state in a dispersive medium with a barrier.*

# Phase-Space Approach to Nonlinear Oscillator Under Periodic Electric Field

Dariusz M. Woźniak and Bartłomiej J. Spisak  
*AGH University of Science and Technology*  
*Faculty of Physics and Applied Computer Science*  
*al. Mickiewicza 30, 30-059 Kraków, Poland*  
*bjs@agh.edu.pl*

The dynamics of classical systems is seldom governed by the linear Hamilton equations. In many cases these equations of motion have complicated (nonlinear) form which can be simplified by a proper coordinates transformation. Probably, the most important types of this transformation concerning integrable systems is the action-angle transformation which reduces given problem to the first-order differential equation and it provides the effective Hamilton function which is independent of the generalized position [1]. An application of this transformation to the anharmonic oscillator placed in a time-dependent electric field leads to description of this perturbed systems in the form of the standard Hamilton function [2]. Quantization of this problem poses a challenge because of the definition of the operators for action and angle variables are ambiguously specified [3].

In this report the Wigner distribution function of the angle and action variables is considered for the nonlinear oscillator system guided by periodic, electric field [4]. For this purpose the eigenvalue problem for the Mathieu equation is numerically solved. As a result, the energies and corresponding eigenfunctions are determined. Then, the eigenfunctions are used to construct the appropriate Wigner distribution functions which are defined by formula [5]

$$q_n(\alpha, I) = \frac{1}{2\pi} \int_{-\pi}^{\pi} d\theta \psi_n^* \left( \alpha - \frac{\theta}{2} \right) \psi_n \left( \alpha + \frac{\theta}{2} \right) e^{-i\theta I},$$

where  $\alpha$  is the angle coordinate varying from  $-\pi$  to  $\pi$ ,  $I$  is the action coordinate, and  $\psi_n(\cdot)$  is the  $n$ -th eigenfunction of the Mathieu equation with fixed parity.

Additionally, the nonclassical properties of these states are analysed in the phase space generated by the angle and action variables.

[1] V.I. Arnold, *Mathematical Methods of Classical Mechanics* (Springer, 2013)

[2] S. Usikov, *Nonlinear Physics*. (Taylor & Francis, 1988)

[3] H. A. Kastrup, Phys. Rev. A 73, 052104 (2006)

[4] A. Ugulava *et al.*, Phys. Rev. E 84, 046606 (2011)

[5] H. A. Kastrup, Phys. Rev. A 94, 062113 (2016)

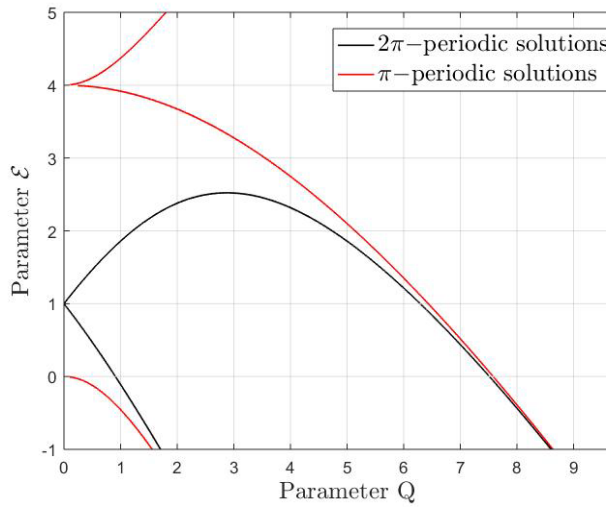


Fig.1: Stability diagram for the Mathieu equation.

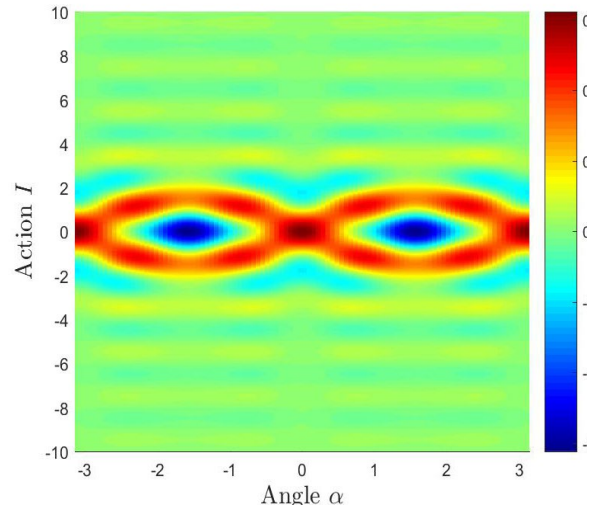


Fig.2: Wigner function for the first even eigenstate.

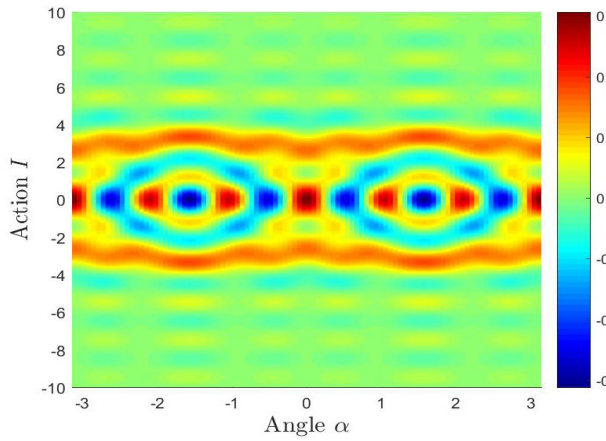


Fig.4: Wigner function for the third even eigenstate.

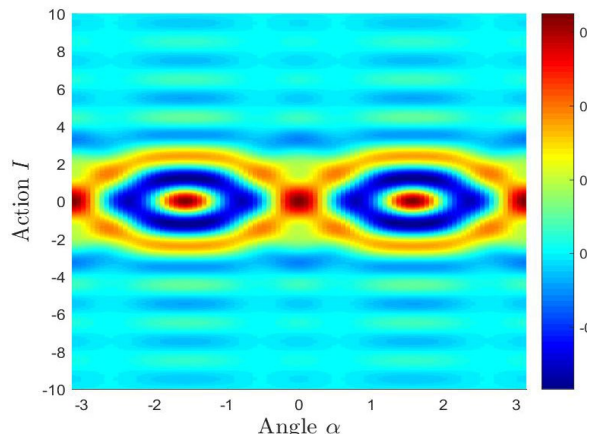


Fig.3: Wigner function for the second even eigenstate.

# Towards Quantum Tomography with Subcycle Temporal Resolution

Andrey S. Moskalenko

*Department of Physics, KAIST, Daejeon 34141, Republic of Korea*

*moskalenko@kaist.ac.kr*

The quantum nature of light possesses many astonishing properties rendering it a promising candidate for novel spectroscopy methods of complex many body phenomena, quantum information processing and subwavelength lithography. Usually its quantum nature is described in the frequency domain and even for broadband quantum states of light a quasi-continuous-wave picture with a well-defined carrier frequency is still applicable. In this picture the Wigner function is used for a phase-space visualization of the states as well as for accessing their physical properties via the classical averaging of the corresponding quantities over the phase space. Extending this approach to pulsed ultrabroadband quantum light would lead to a quite involved description in terms of a large set of single-frequency or shaped temporal modes, where each mode has to be characterized separately. An alternative approach is to consider the quantum fields directly in the time domain. For example, considering the time-resolved behavior of the photonic ground state one can show that vacuum fluctuations of its electric field can be detected using the linear electro-optic effect [1,2]. In the corresponding setup a few-femtosecond near-infrared probe pulse is sent through a thin electro-optic crystal where it interacts with the vacuum in the mid-infrared (MIR) range and then analyzed. Furthermore, it is possible to formulate a consistent time-domain theory of the generation and time-resolved detection of few-cycle and subcycle pulsed squeezed states [3].

A slightly modified version of the setup enables the detection of the probability distribution of the analyzed probe field for arbitrary phase shifts, thus enabling a full quantum tomography of its state [4]. This should pave the way to the extraction of the phase-space distributions of the sampled MIR field with an extreme (subcycle) temporal resolution. For that a procedure to disentangle the contributions of the MIR field from the NIR quantum shot noise has still to be found. Alternatively, we propose how to retrieve the subcycle-resolved Wigner function based on the homodyne detection with phase-controlled half-cycle pulses and illustrate this for the pulsed squeezed vacuum states.

[1] C. Riek *et al.*, Science 350, 420 (2015)

[2] A.S. Moskalenko *et al.*, Phys. Rev. Lett. 115, 263601 (2015)

[3] M. Kizmann *et al.*, Nat. Phys. 15, 960 (2019)

[4] M. Kizmann *et al.*, arXiv:2103.07715 (2021)



# High-Order Harmonics Radiation and its Time-Frequency Wigner Representation for a Two-Level System Driven by Ultrashort Pulses

Seongjin Ahn and Andrey S. Moskaleiko

*Department of Physics, KAIST, Daejeon 305-701, Korea*

*seongjin.ahn@kaist.ac.kr*

The dynamics and time-dependent radiation spectra of a model two-level system driven by ultrashort half- and single-cycle pulses have been investigated. We find that the expectation value of the induced dipole moment starts to exhibit extremely rapid oscillations if the driving pulse reaches certain strength, so that this system can then serve as a light source with much higher frequencies than the input pulse. To understand the underlying mechanism in view of possible applications, we utilize a unitary perturbation theory capable to address interactions with strong ultrashort ultrabroadband pulses [1]. Based on this theory we obtain a fully analytical expression for time-dependent electronic state and radiation spectra. We have also identified a set of frequencies at which the radiation is suppressed by orders of magnitude and studied their behavior as a function of pulse strength and duration, enabling quantitative control over the spectra, with potential applications such as attosecond pulse generation. Finally, we have analyzed the emitted electric field in the time-frequency domain using the Husimi and Wigner functions [2]. Comparing with the Husimi function, the representation of the spectra via the Wigner function uncovers interference fringes, sensitive to the strength of the driving field. This allows for distinguishing between even slightly different emitted light pulses. Along with its experimental realizability [3], this capability can be potentially exploited for quantum information processing.

[1] A.S. Moskaleiko *et al.*, Phys. Rep. 672, 1-82 (2017)

[2] L. Praxmeyer *et al.*, Phys. Rev. Lett. 98, 063901 (2007); E. Wigner, Phys. Rev. Lett. 40, 749 (1932)

[3] L. Praxmeyer *et al.*, Phys. Rev. A 93, 053835 (2016)

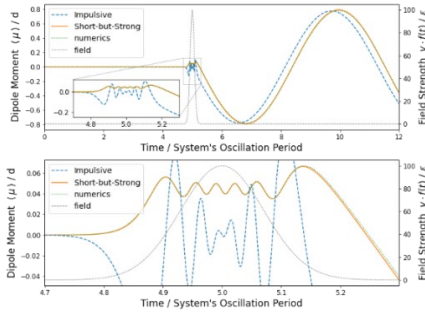


Fig.1: Dipole moment of the two-level model system driven by a half-cycle pulse. The analytical expression according to Impulsive approximation, Short-but-Strong approximation, and numerical results are plotted.

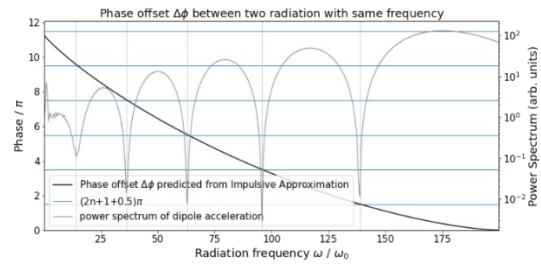


Fig.4: A radiation spectrum by a half-cycle driving field is shown along with the frequencies at which 'dips' occur. Those frequencies are identified where the phase difference between the two radiation fields of the same frequency have a fixed offset.

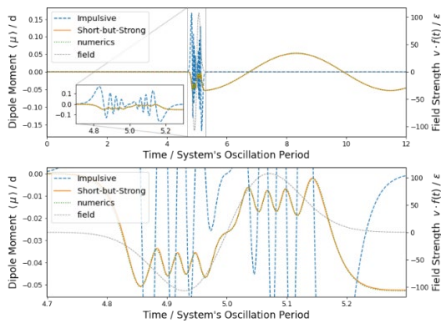


Fig.2: Same as Fig 1, except using a single-cycle pulse as the driving field.

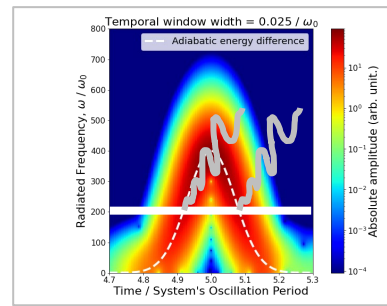


Fig.5 Time-windowed Fourier transformation to show two different radiation for each given radiation frequency.

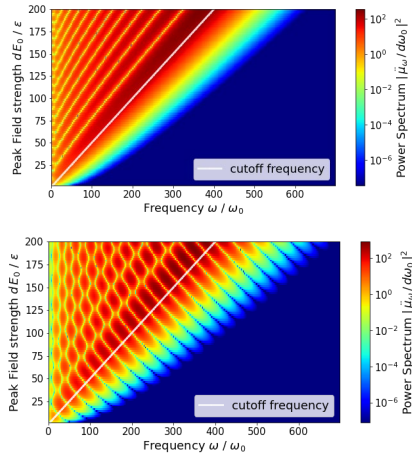


Fig.3: On the upper plane is the radiation spectra for each field strength of the driving field in case of a half-cycle pulse. The lower plane is the same except that the driving field is a single-cycle pulse.

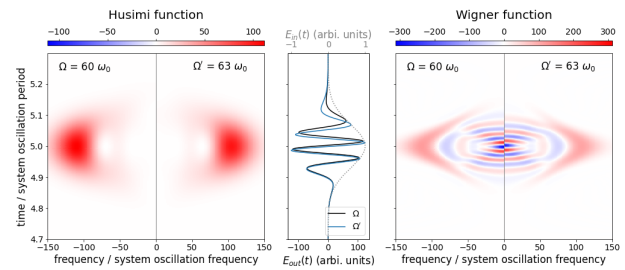


Fig.6: Husimi (left) and Wigner functions (right) corresponding to emitted electric fields (center) from the two-level system driven by two different strengths of external fields, expressed in terms of Rabi frequencies  $\Omega = 60\omega_0$  and  $\Omega' = 63\omega_0$  where  $\omega_0$  is the transition frequency between the two levels. The low frequency parts of the Wigner functions are sensitive to the change of external field strengths, as compared to the information provided by the Husimi functions.

# Thermodynamic Properties of Unpolarized Uniform Electron Gas: Monte Carlo simulations

Alexander Larkin<sup>1</sup>, Vladimir Filinov<sup>1</sup>, and Pavel Levashov<sup>1,2</sup>

<sup>1</sup>*Joint Institute for High Temperature RAS, Russia*

<sup>2</sup>*Moscow Institute of Physics and Technologie, Russia*

*alexanderlarkin@rambler.ru*

The uniform electron gas (UEG) at finite temperature is one of the simplest and, in the same time, one of the most important non-ideal many-body quantum system. Consisting of the negative-charged electrons and the rigid positive-charged background, UEG is the simplified model of warm dense matter used in physics of dense plasma, laser-excited solids, etc.. Thermodynamic state of UEG can be described with two dimensionless parameters: degeneracy parameter  $\theta=kT/E_F$  and density parameter  $r_S=r/a_0$ , where  $r$  is Wigner-Seitz radius.

In the warm dense matter regime, when the system is significantly degenerate and non-ideal ( $\theta<5$ ,  $r_S>0.5$ ), perturbation theory is not working and numerical simulations are required. The existing path integral Monte Carlo methods for UEG, based on the partition function in coordinate representation, in are insufficient yet. The first reason is famous fermionic sign problem even at moderate degeneracy. The second reason is inability to calculate some thermodynamical values and functions, as momentum distribution functions, average potential or kinetic energies, which are required for many kinetic applications.

We present a new Monte Carlo method for simulations of UEG, based on path integral representation of the Wigner function. This method can calculate momentum- and coordinate-depending thermodynamic separately, including the distribution functions. The fermionic sign problem is significantly reduced by using exchange determinants.

We used our method to numerical simulations of unpolarized UEG in range of states  $0.5<\theta<4$ ,  $0.2<r_S<8$ . We have studied the next thermodynamic properties: average potential energy, average kinetic energy, full energy, exchange-correlation energy, pair correlation functions and momentum distribution functions. This results are in quite good agreement with available data for UEG and expand and clarify results of the existing path integral Monte Carlo methods. Some of these results are shown on the figures.

**Acknowledgements.** The theoretical approach to the basic equations was supported by the Russian Science Foundation, Grant No.20-42-04421. The algorithmic realization of the approach was supported by the subsidy for a large scientific project in priority areas of scientific and technological development No.13.1902.21.0035. The numerical calculations have been supported by the State assignment No.075-00892-20-00.

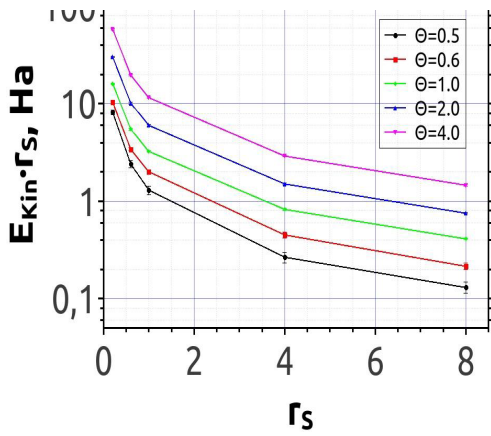


Fig.1: Average kinetic energy of unpolarized UEG per electron for different values of  $r_s$  and  $\theta$ .

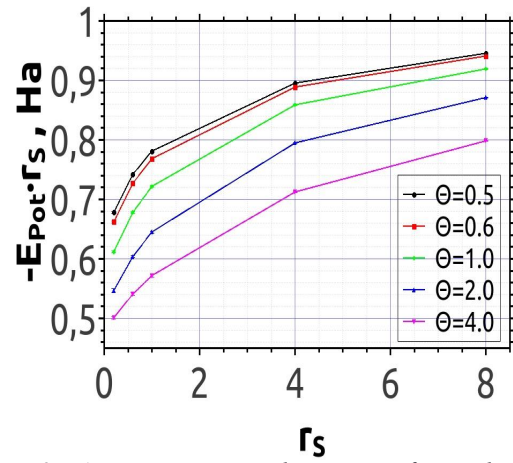


Fig.2: Average potential energy of unpolarized UEG per electron for different values of  $r_s$  and  $\theta$ .

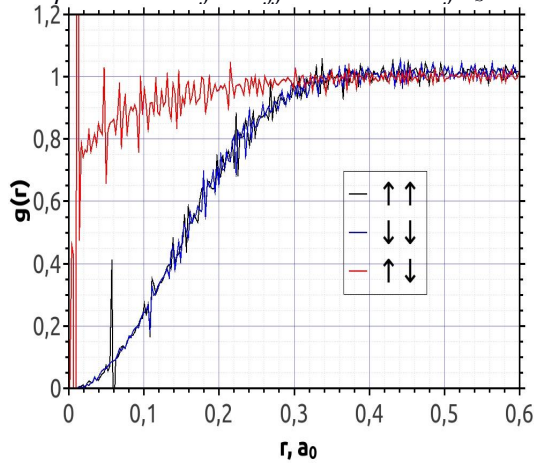


Fig.3: Pair correlation functions of unpolarized UEG for  $r_s=0.2$ ,  $\theta=0.5$  (degenerate, weakly non-ideal).

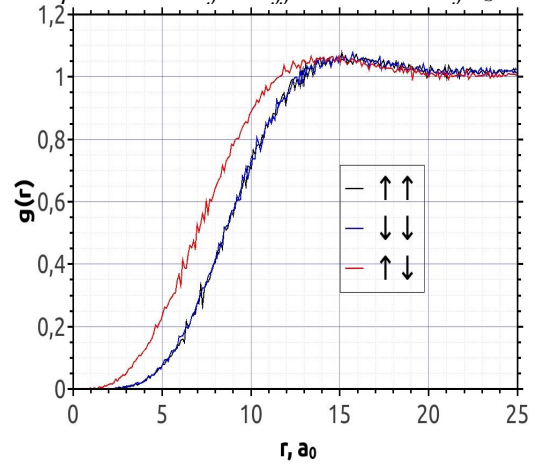


Fig.4: Pair correlation functions of unpolarized UEG for  $r_s=8.0$ ,  $\theta=0.5$  (degenerate, strongly non-ideal).

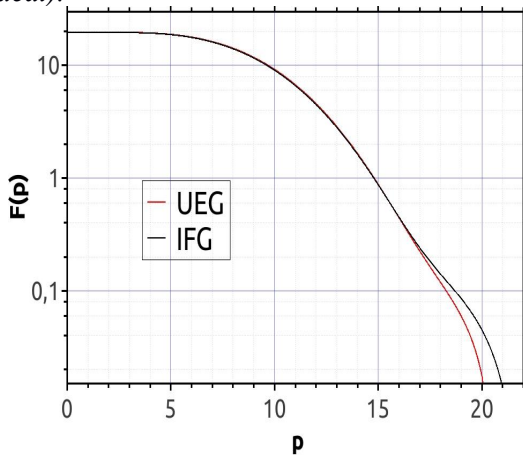


Fig.5: Momentum distribution function of unpolarized UEG for  $r_s=0.2$ ,  $\theta=0.5$  (degenerate, weakly non-ideal), compared with ideal Fermi gas.

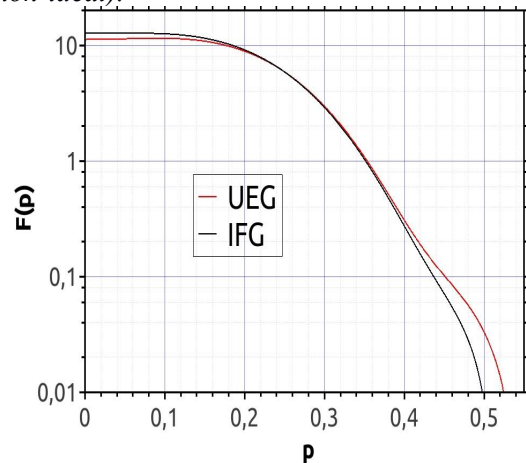


Fig.6: Momentum distribution function of unpolarized UEG for  $r_s=8.0$ ,  $\theta=0.5$  (degenerate, strongly non-ideal), compared with ideal Fermi gas.

# A Time-Frequency Approach to Relativistic Correlations in Quantum Field Theory

Benjamin Roussel and Alexandre Feller

*Advanced Concepts Team, European Space Agency, Noordwijk, 2201 AZ, Netherlands*

*benjamin.roussel@aalto.fi*

Moving detectors in relativistic quantum field theories reveal the fundamental entangled structure of the vacuum. This is illustrated by the so-called Unruh effect [1], in which uniformly-accelerated detectors in the vacuum see a thermal state. In this talk, I propose a general formalism inspired both from signal processing and correlation functions of quantum optics to analyze the response of point-like detectors following a generic, non-stationary trajectory [2]. In this context, the Wigner representation of the first-order correlation of the quantum field is a natural time-frequency tool to understand single-detection events. This framework offers a synthetic perspective on the problem of detection in relativistic theory and allows us to analyze various non-stationary situations (adiabatic, periodic) and how excitations and superpositions are deformed by motion. It opens up interesting perspective on the issue of the definition of particles.

[1] W. G. Unruh, Phys. Rev. D. 14 (4), 870 (1976)

[2] B. Roussel, A. Feller, Phys. Rev. D 100, 045016 (2019)

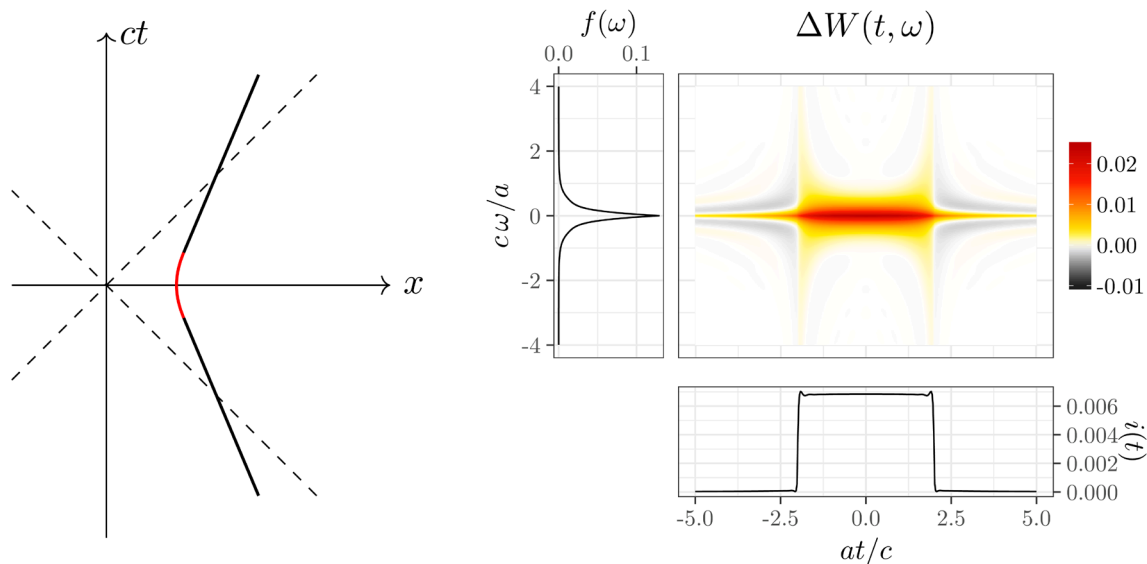


*Fig.2: Left pannel: space-time trajectory followed by an observer that is accelerated during a finite time. The accelerated portion is in red. Right pannel: Wigner function and marginal of the bosonic field perceived by the accelerated observer in its proper time. The trajectory is accelerated from  $t = -2a/c$  to  $t = 2a/c$ . We can see on the time marginal the instant response in the acceleration.*



# Using Classical Wigner Dynamics to Elucidate Tunneling Times

Tom Rivlin<sup>1</sup>, Eli Pollak<sup>1</sup>, and Randall Dumont<sup>2</sup>

<sup>1</sup>*Chemical and Biological Physics, Weizmann Institute of Science, 76100 Rehovot, Israel*

<sup>2</sup>*Chemistry & Chemical Biology, McMaster University, Hamilton, Ontario, Canada L8S 4M1*

*tom.rivlin@weizmann.ac.il*

There are many outstanding debates surrounding the issue of time in quantum tunneling [1–5], including debates over how much time a particle spends inside a barrier when it tunnels. Many of these debates stem from concerns over the shapes of the wavepackets involved in the tunneling process, and how the process changes them. The use of Wigner functions [6] in tunneling time calculations has the potential to resolve many of these issues [7]. In this presentation, and as described in Ref. [8], we use Wigner dynamics as an unambiguous reference point to unravel the quantum tunneling time, which is masked by a momentum-filtering effect. We do this by comparing time propagation for classical Wigner and numerically exact quantum distributions. The classical Wigner scheme is set up with the assumption that the tunneling time vanishes, yet the momentum-filtering effect is built into it rather accurately. The quantum mechanical flight time is then found to be longer than the classical Wigner flight time, and this added time reflects the actual tunneling time. These comparisons have produced clear, explicit demonstrations that the time taken to traverse a square barrier is precisely the reflected phase time (sometimes called the Wigner time [9]). That the two are equal suggests that the tunnel traversal time is a finite quantity that is almost entirely independent of the width of the barrier, verifying the curious phenomenon commonly known as the Hartman effect [10, 11].

**Acknowledgements.** This work was supported by grant 408/19 of the Israel Science Foundation.

- [1] E. Hauge, J. Støvneng, *Rev. Modern Phys.* 61, 917 (1989)
- [2] R. Landauer, *Berich. Bunsengesell. Phys. Chem.* 95, 404 (1991)
- [3] S. Brouard *et al.*, *Phys. Rev. A* 49, 4312 (1994)
- [4] C. McDonald *et al.*, *J. Phys. Conf. Ser.* 594, 01201 (2015)
- [5] H. G. Winful, *Phys. Rep.* 436, 1 (2006)
- [6] E. J. Heller, *J. Chem. Phys.* 65, 1289 (1976)
- [7] J. Muga *et al.*, *Phys. Lett. A* 167, 24 (1992)
- [8] T. Rivlin *et al.*, *Phys. Rev. A* 103, 012225 (2021)
- [9] E. Wigner, *Phys. Rev.* 40, 749 (1932)
- [10] T. E. Hartman, *J. Appl. Phys.* 33, 3427 (1962)
- [11] J. G. Muga, in *Time in Quantum Mechanics*, edited by J. Muga, R. S. Mayato, I. Egusquiza, p. 31-72. (Springer, 2008)

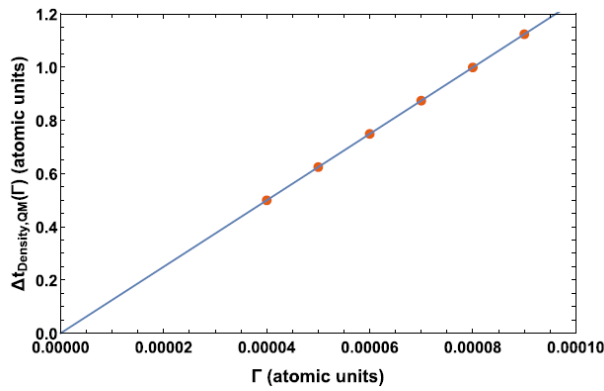


Fig.1: The difference between the reflected and transmitted mean time of flight as a function of the wavepacket width,  $\Delta t_{QM}(\Gamma)$ , for the numerically exact quantum density time distribution.

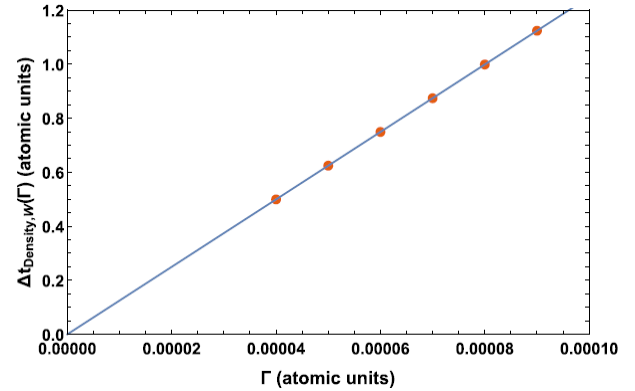


Fig.2 The difference between the reflected and transmitted mean time of flight as a function of the wavepacket width,  $\Delta t_W(\Gamma)$ , for the classical Wigner time distribution.

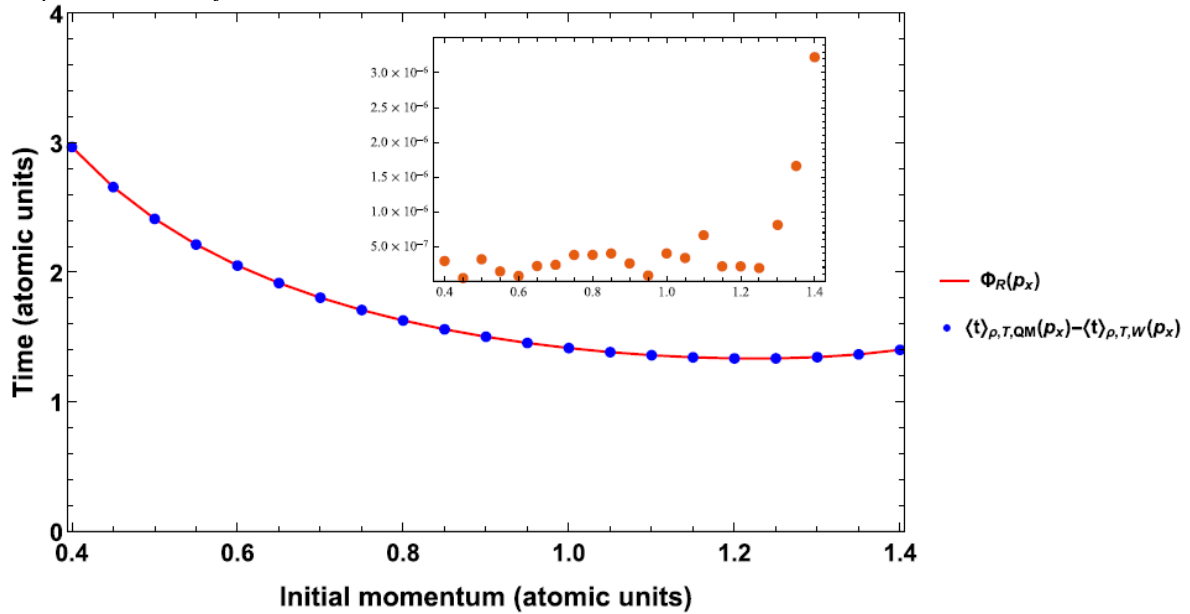


Fig.3: The difference between the  $\Gamma \rightarrow 0$  mean time of flight of the tunneled particle propagated quantum mechanically,  $\langle t \rangle_{QM}$ , and the  $\Gamma \rightarrow 0$  mean time of flight for the classical Wigner-propagated tunneled particle,  $\langle t \rangle_W$ , as a function of the initial momentum  $p_x$  (dots), compared with the reflected phase time  $\Phi_R$  also as a function of  $p_x$  (line), Inset: the relative error.

# Dissipative Phase Space Crystals in Josephson Circuits

Ben Lang and Andrew D. Armour

*School of Physics and Astronomy and Centre for the Mathematics and Theoretical Physics of Quantum Non-Equilibrium Systems, University of Nottingham, Nottingham NG7 2RD, UK*  
*ben.lang@nottingham.ac.uk*

Superconducting Josephson photonic circuits are a powerful platform for the realization of strongly nonlinear quantum systems. One advantage of these systems is that multi-photon resonances can be engineered [1], where photons are produced in handfuls - perhaps as many as 6 or more at a time in currently accessible circuits (fig.1). These multi-photon resonances are very interesting from a phase-space perspective, where the creation of photons in groups of  $p$  maps onto a rotational symmetry of degree  $p$ . The rotational symmetry arising in the Hamiltonians of these systems has been shown to play a role like that of translation in a crystal [2], giving rise to rich periodic structures in phase space known as *phase space crystals*. We study the analogous effects that occur in open quantum circuits where damping and driving must be accounted for via the density operator; in such systems the dynamics is controlled by the Liouvillian, an object that contains both the effects of Hamiltonian evolution and environmental coupling. We explore the evolution of the eigenoperators of the Liouvillian, together with the associated eigenvalues as system parameters are tuned leading to dramatic changes in the system's steady state. We carry out a decomposition of the Liouvillian into a steady state (zero eigenvalue) and transients, tracing the emergence of spectral gaps in the eigenspectrum which allow the behavior to be understood in terms of dissipative phase transitions [3]. We also use Wigner transforms of the eigenoperators (fig.2) as a useful tool for visualization; the non-Hermitian character of the eigenoperators is reflected in complex-valued Wigner transforms [4]. We find that the eigenoperators are described by Bloch modes in phase space (fig.2), and close to a  $p$ -photon resonance each is unchanged by a discrete rotation of  $2\pi/p$ , up to a phase  $\exp(ik)$ , with  $k$  playing the role of wavenumber. For appropriate tuning of the system parameters, we find that the dissipative phase space crystal can even be made diatomic, leading to an optical and an acoustic band separated by bandgap.

[1] B. Lang, A. D. Armour, arXiv:2012.10149 (2020)

[2] L. Guo *et al.*, Phys. Rev. Lett. 111, 205303 (2013)

[3] F. Minganti *et al.*, Phys. Rev. A 98, 042118 (2018)

[4] H.J. Groenewold, Physica 12(7), 405-460 (1946)

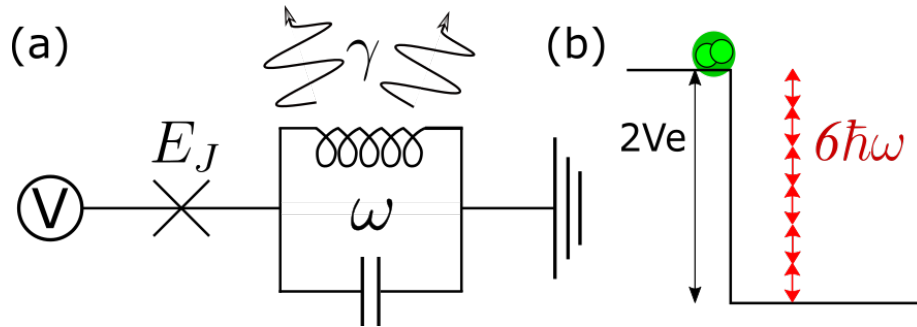


Fig.1: (a) Superconducting circuit system: a DC voltage source together with a Josephson junction drives an electromagnetic cavity mode, which leaks photons into the environment. (b) The voltage is set so that 6 photons are generated by the tunneling of each Cooper pair through the circuit.

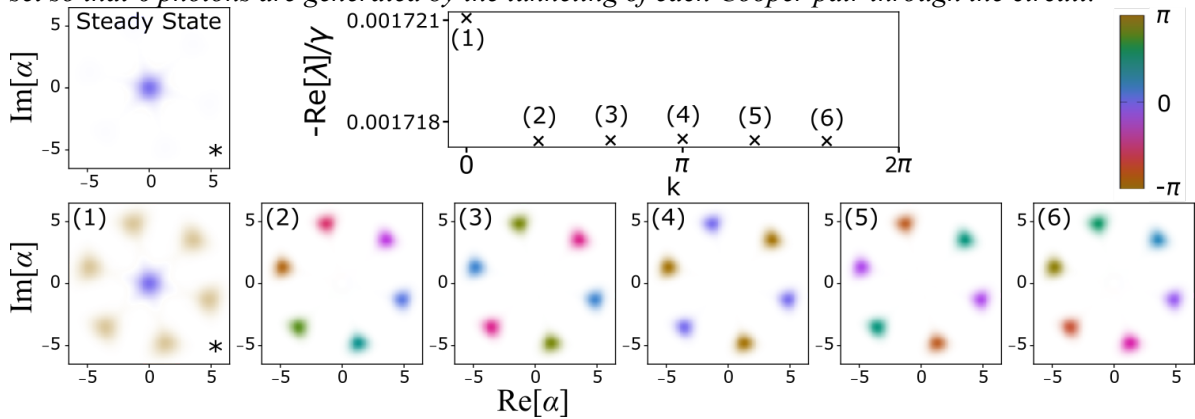


Fig.2: Top Right: Band diagram, showing the slow decay time of some eigenoperators as a function of their rotational symmetry (encoded by  $k$ ). Also shown are Wigner functions of the eigenoperators for the steady-state and the decaying modes with corresponding eigenvalues labelled in the band diagram. In these plots the hue indicates the phase whilst the intensity gives the amplitude. In the plots with (\*)s the amplitude is scaled by  $1/2$  to enhance weaker features. The blobs in the Wigner functions coincide with the classical fixed points of the system (7 in this case).

# Selective Correlations in Finite Quantum Systems: The Desargues and Pappus Properties

Ci Lei and Apostolos Vourdas

*Department of Computer Science, University of Bradford, UK*

*clei1@bradford.ac.uk*

The Desargues and Pappus properties are well known in projective geometry. We show that there are analogous properties in the context of both classical and quantum physics. The Desargues property can be interpreted classically using two logical circuits with the same input and showing selective correlation in the outputs. In the context of quantum physics, the Desargues property can be interpreted in terms of selective quantum correlation. We also studied the Pappus property and presented its translation in a quantum context. The formalism is in terms of projectors and can also be expressed in terms of Q, P and Wigner functions. The work shows that there are deep links between quantum mechanics and projective geometry.

[1] C.Lei, A.Vourdas, J. Phys. Conf. Series. 1194, 012069 (2019)

[2] C.Lei, A.Vourdas, J. Geom. Phys. 128, 118 (2018)

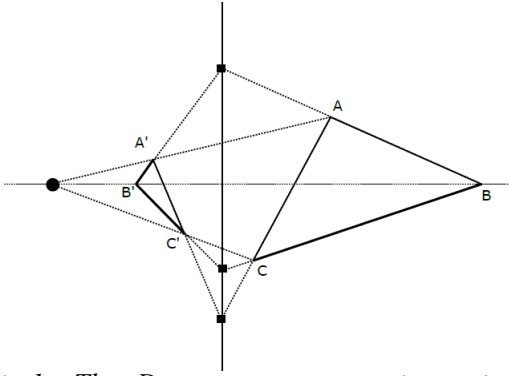


Fig.1: The Desargues property in projective geometry.

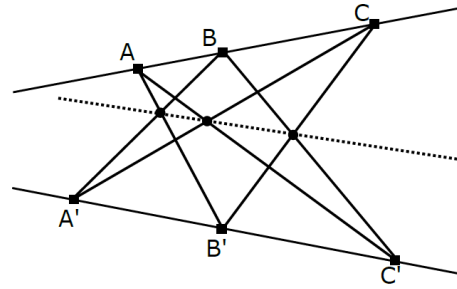


Fig.2: The Pappus property in projective geometry.

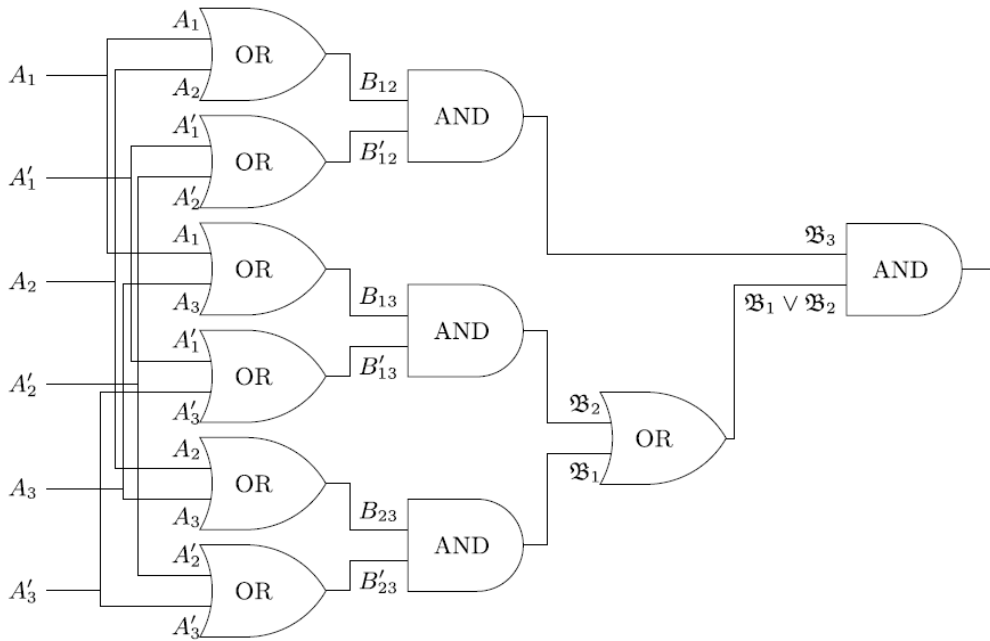
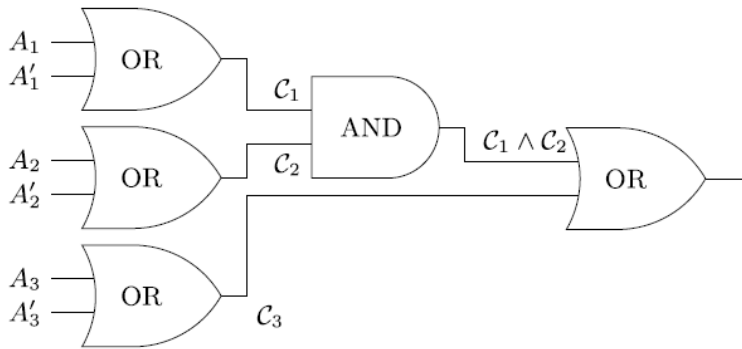


Fig.3: The Desargues property in Boolean algebra.

# Thermoelectric Transport in Nanostructured Materials: The Wigner-Boltzmann Approach

Zlatan Aksamija and Adithya Kommini

*University of Massachusetts Amherst, Amherst, MA 10135, USA*

*zlatana@umass.edu*

The impact of quantum transport on the thermoelectric (TE) properties of nanostructures has been of great scientific and practical interest in recent years, especially since early theoretical work showed that reduced size or dimensionality can induce significant gains in TE efficiency. Potential barriers by band offsets (in superlattices) or external potentials (by gating) can dramatically enhance the TE power factor through energy filtering or confining the carriers. However, since TE devices are typically “nanostructure-in-bulk” rather than a single, isolated nanostructure between contacts, their TE properties depend simultaneously on semi-classical (electron-phonon, impurity, and boundary scattering) and quantum (tunneling through potential barriers) effects. Including both in a comprehensive simulation tool has proven challenging. In this work, we perform extensive numerical simulations combining first-principles electronic structure with a Wigner-Boltzmann solver for transport. This formalism is based on the Wigner transform to capture the full effect of the potential barriers on carrier quantum transport, while the collision term from the Boltzmann transport equation captures the semi-classical effects such as phonon and impurity scattering.

Two-dimensional (2D) materials are of great interest for next-generation energy solutions by allowing improved thermoelectric (TE) conversion performance while offering gate-tunable power factors and flexible structure that can be integrated into wearables and health monitoring devices. While there have been numerous recent papers identifying novel 2D materials as potential candidates for high intrinsic thermoelectric performance, there have been far fewer papers putting forth a comprehensive analysis of how and to what extent can the TE performance be further extrinsically enhanced. The possibility of creating such structures in 2D by lateral superlattices, periodic gates, alloying, or substrate patterning to modulate the bandgap have all been experimentally demonstrated in other contexts, but the impact of such approaches on 2D TEs remains largely an open question. We validate our results against intrinsic MoS<sub>2</sub> experimental data, then deploy this formalism on a broad swath of potential barrier shapes, heights, and periods to elucidate those conditions that lead to improved TE performance. The conclusions we draw point to ways to optimize nanostructures for TE applications and have impact on nanocomposites, which have potential barriers at grain boundaries and are widely employed to boost TE efficiency of materials.



# Exceptional Points from the Hamiltonian of a Hybrid Physical System

Marta Reboiro<sup>1</sup>, Romina Ramírez<sup>2</sup>, and Diego Tielas<sup>3</sup>

<sup>1</sup>*IFLP, CONICET-Department of Physics, National University of La Plata*

<sup>2</sup>*Department of Mathematics, National University of La Plata*

<sup>3</sup>*IFLP, CONICET-CONICET-Faculty of Engineering, National University of La Plata*  
*reboiro@fisica.unlp.edu.ar*

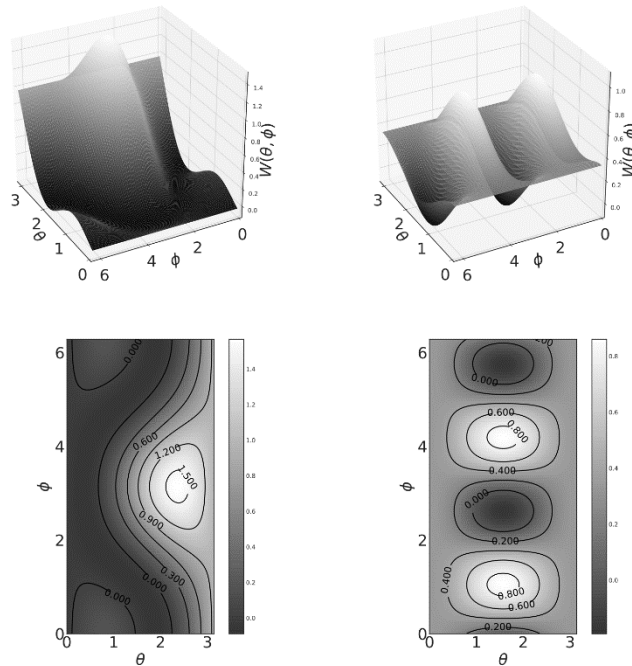
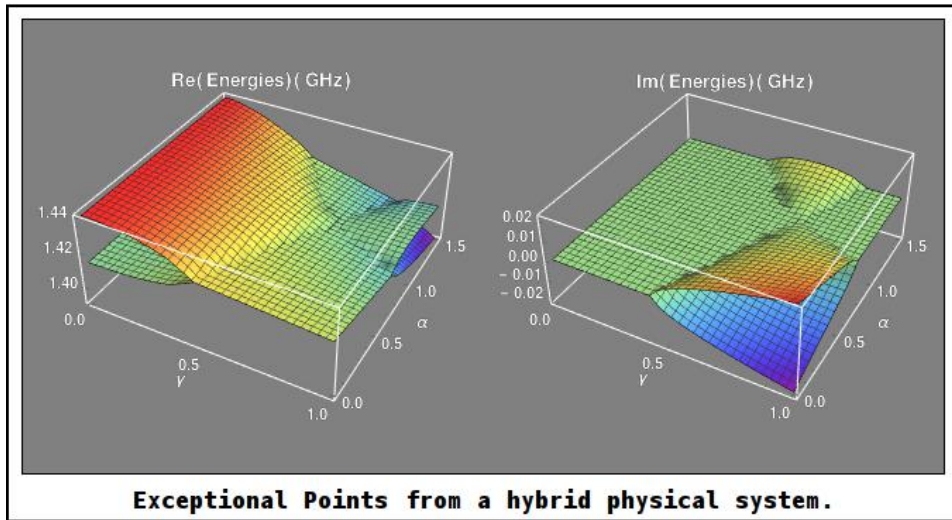
We study the appearance of Exceptional Points in a hybrid system composed of a superconducting flux-qubit and an ensemble of nitrogen-vacancy color centers (NVs) in diamond [1]. We have modeled the dynamics of the system through a non-hermitian Hamiltonian, to take into account the effect of the environment on the ensemble of NVs. Though the Hamiltonian does not preserve  $PT$ -symmetry, the spectrum consists of real eigenvalues or complex-conjugate pair eigenvalues, and it shows the characteristic features of a system with gain-loss balance. We discuss the possibility of controlling the generation of Exceptional Points, by the analysis of the model space parameters. One of the characteristic features of the presence of Exceptional points is the departure from the exponential decay behavior of the observables as a function of time. The study of the matrix elements of the Fourier Transform of the Green Matrix provides information on the transition probabilities of the states of the original base as a function of time. Thus, we can prepare robust initial states by combining the states which show large transition probabilities at long intervals of time. It is observed that in the regime of real spectrum, the initial state evolves in time showing a periodical pattern of collapses and revivals. In this regime, the states are periodically squeezed. While in the regime of complex-conjugate pair spectrum the steady-state is not a squeezed state, and anti-squeezing is observed. For certain values of model space, the steady anti-squeezed steady-state has mean value of the total spin of the NVs equals zero. At these values, we have shown the presence of Schrödinger spin cat states, that is states which are a superposition of two coherent spin states. We have extended the previous analysis to systems with a larger number of NV<sup>-</sup>-color-centers in diamond and we have found a regular pattern of Exceptional Points and a regular pattern of steady Schrödinger spin cat states.

Work is in progress concerning the analysis of hybrid systems with more than one superconducting flux qubit, interacting with an ensemble of NVs.

[1] R. Ramírez *et al.*, Eur. Phys. J. D, 74, 193 (2020);

Europhys. News 51(5), (2020) <http://www.eorophysicsnews.org/vol-51-no-5-highlights>**Error!**

**Hyperlink reference not valid.**



*Discrete Wigner Function  $W$  of the NV-color-centers. In the left panels we display the behavior of  $W$  for the Initial State and in the left ones in the steady-state. Initially, the superconducting qubits are prepared in its ground state, and the NVs in a coherent state.*

# **Orientalional Order Parameters for Arbitrary Quantum Systems**

Michael te Vrugt and Raphael Wittkowski

*Institut für Theoretische Physik, Center for Soft Nanoscience, Westfälische Wilhelms-Universität Münster, D-48149 Münster, Germany*  
*raphael.wittkowski@uni-muenster.de*

Classical liquid crystals are known to exhibit a variety of orientational phases, which are measured using order parameters such as the polarization vector and the nematic tensor. These are obtained from an angular or Cartesian multipole expansion of the one-body distribution function of the liquid crystal [1]. More recently, nematic phases were observed in so-called “quantum liquid crystals”. Quantum nematic order is now important in the theory of superconductivity or ultracold atomic gases. However, it is technically difficult to relate angular and Cartesian definitions of order parameters in practice, and it is unclear how the method of orientational expansions can be applied to quantum systems.

We generalize the classical theory of order parameters to quantum mechanics based on an expansion of Wigner functions. This provides a unified framework applicable to arbitrary quantum systems [2]. The formalism recovers the standard definitions for spin systems. For Fermi liquids, the formalism reveals the nonequivalence of various definitions of the order parameter used in the literature. Moreover, new order parameters for quantum molecular systems with low symmetry are derived, which cannot be properly described with the usual nematic tensors.

[1] M. te Vrugt, R. Wittkowski, *AIP Adv.* 10, 035106 (2020)

[2] M. te Vrugt, R. Wittkowski, *Ann. Phys. (Berl.)* 532, 2000266 (2020)



# Wigner Function and Entropy Dynamics of a Single Phonon Mode Coupled to an Optically Excited Quantum Dot

Thilo Hahn<sup>1,2</sup>, Daniel Wigger<sup>2</sup>, and Tilmann Kuhn<sup>1</sup>

<sup>1</sup>*Institute of Solid State Theory, University of Münster, Germany*

<sup>2</sup>*Department of Theoretical Physics, Wrocław University of Science and Technology, Poland*  
*t.hahn@wwu.de*

Entropy is a fundamental concept in physics. Under thermal equilibrium conditions the realized state of a system maximizes the entropy. While in a closed system under nonequilibrium conditions its decrease is prohibited by the second law of thermodynamics, the entropy of a subsystem interacting with its environment may decrease. The study of the subsystem's entropy dynamics therefore provides valuable information on the evolution of the system's quantum state. In particular, the linear entropy  $\text{Tr}(\rho - \rho^2)$  is directly related to the purity of a state [1].

We consider a quantum dot (QD) modeled as a two-level system, which interacts with a single phonon mode via the pure dephasing coupling. We investigate the phonon dynamics after ultrafast optical excitations of the QD exciton by using a Wigner function formalism. The exciton-phonon coupling leads to a shift in the equilibrium position of the lattice ions in phase space. In the subspace associated with the QD ground state  $|g\rangle$ , the equilibrium position in phase space is the origin, while in the subspace associated with the excited state  $|x\rangle$  it is shifted by twice the dimensionless exciton-phonon coupling strength  $\gamma$ . The Wigner function not only gives insight into the phase space dynamics but it is also directly connected to the linear entropy allowing for a detailed interpretation of the dynamics.

We find that the decay of the excited state occupation leads to non-trivial phonon dynamics in phase space, depending on the ratio between the decay rate  $\Gamma$  and the phonon frequency  $\omega_{\text{ph}}$  [2]. The Wigner function after a complete decay into the QD ground state is shown in Fig. 1a for different ratios of  $\Gamma/\omega_{\text{ph}}$ . On the one hand, if the decay occurs very fast, the Wigner function hardly differs from the one of the vacuum state. On the other hand, when the decay is much slower than the phonon frequency it becomes ring-shaped. In between, if the decay occurs on the same timescale as the phonon frequency, the Wigner function exhibits a tail-shaped structure. The corresponding dynamics of the entropy of the phonon subsystem are shown in Fig. 1b. A slow decay leads to a higher linear entropy of the phonon system and shows additional features like a temporary decrease due to self-overlap of the Wigner function, which can be traced back to a loss of entanglement entropy (Fig. 1c) [3].

A more involved decay scenario is observed in the case of the decay of a Schrödinger cat state, which is displayed in Fig. 1d. In addition to the decay of the coherent states, the temporal evolution of the interferences leads to involved phase space and entropy dynamics which we will discuss.

[1] J. Eisert *et al.*, Rev. Mod. Phys. 82, 277 (2010)

[2] T. Hahn *et al.*, Phys. Rev. B 100, 5 (2019)

[3] T. Hahn *et al.*, Entropy 22, 286 (2020)

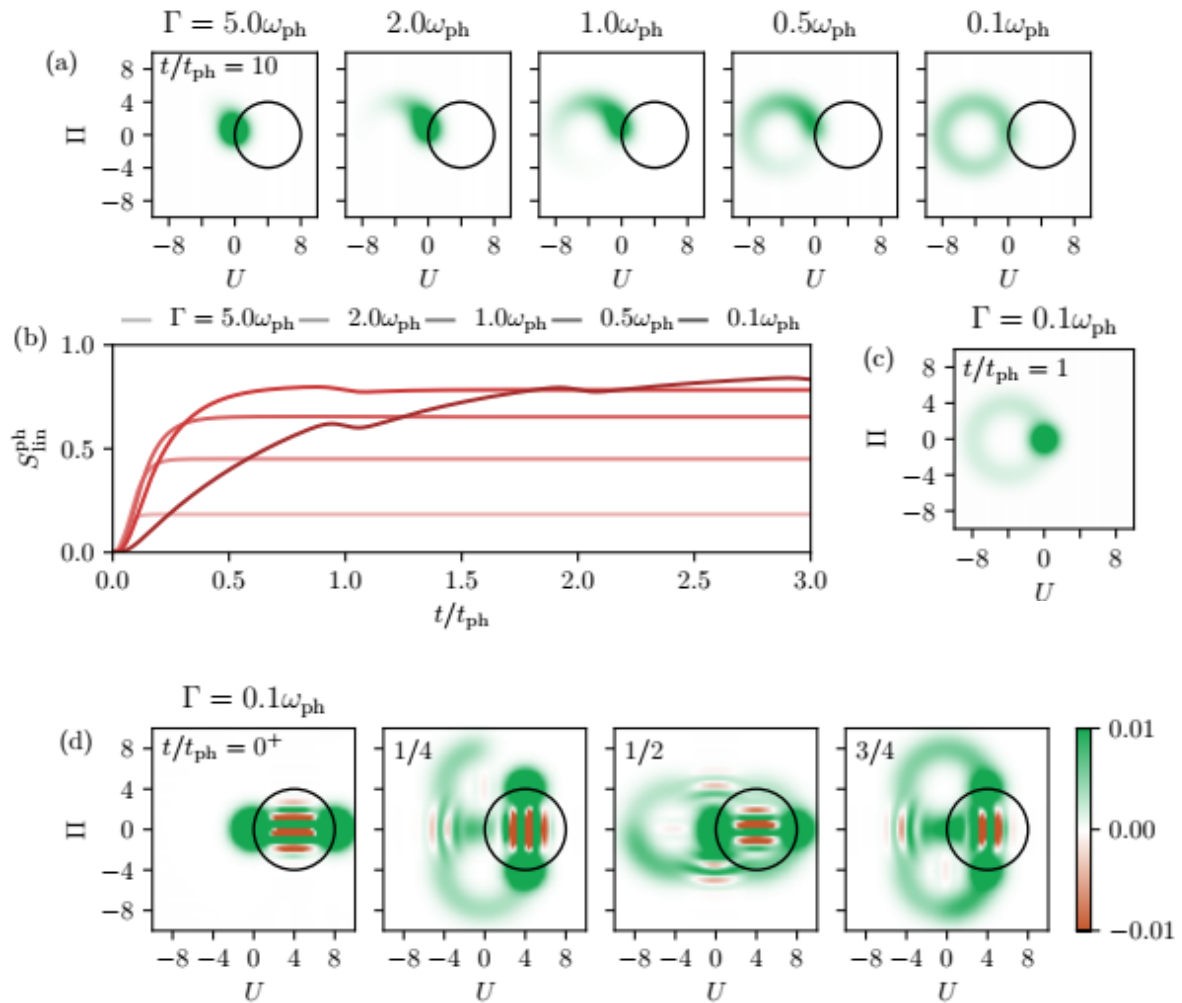


Fig. 1: (a) Phonon Wigner function after excitation and full decay of the QD for different decay rates. (b) Linear phonon entropy dynamics after the optical excitation. (c) Exemplary Wigner function for a slow decay rate after one period. (d) Decay dynamics of the Wigner function of a cat state prepared in the subspace of the QD excited state [3].

# Wigner Ensemble Monte Carlo Simulation Without Discretization Error of a GaAs Resonant Tunneling Diode

Orazio Muscato

*Dipartimento di Matematica e Informatica, Università di Catania, Italy*

*orazio.muscato@unict.it*

The Wigner transport equation represents a promising model for the simulation of electronic nanodevices, which allows the comprehension and prediction of quantum mechanical phenomena in terms of quasi distribution functions. During these years, a Monte Carlo technique for the solution of this kinetic equation has been developed, based on the generation and annihilation of signed particles [1]. The development of Monte Carlo algorithms for this quantum kinetic equation have been tackled, using a probabilistic model based on a particle system with the time evolution of a piecewise deterministic Markov process [2]. Each particle is characterized by a real-valued weight, a position, and a wave-vector. The particle position changes continuously, according to the velocity determined by the wave-vector. New particles are created randomly and added to the system. The main result is that appropriate functionals of the process satisfy a weak form of the Wigner equation. Moreover, a stochastic algorithm without time discretization error can be introduced [3]. This is a rather pleasant feature, since the problem of choosing an appropriate time step is avoided and, in many cases the no-splitting algorithm is more efficient compared to time-splitting algorithms. Simulation results shall be presented during the conference, where standard analytical band scattering model used for the simulated RTD includes polar optical and acoustic deformation potential scattering, assuming parameter values for GaAs.

[1] M. Nedjalkov *et al.*, Phys. Rev. B 70, 115319 (2004)

[2] O. Muscato, W. Wagner, SIAM J. Sci. Comput 38(3), A1438-A1507 (2016)

[3] O. Muscato, W. Wagner, Kin. Rel. Models 12(1), 59-77 (2019)



# Quantum Transmission Conditions for the Simulation of Graphene Heterojunction Devices

Luigi Barletti<sup>1</sup>, Giovanni Nastasi<sup>2</sup>, Claudia Negulescu<sup>3</sup>, and Vittorio Romano<sup>2</sup>

<sup>1</sup>*Dipartimento di Matematica e Informatica “U. Dini”, Università di Firenze, Italy*

<sup>2</sup>*Dipartimento di Matematica e Informatica, Università di Catania, Italy*

<sup>3</sup>*Institut de Mathématiques de Toulouse, Université Paul Sabatier, Toulouse, France*

*luigi.barletti@unifi.it*

In graphene-based electronic devices, the “heterostructures” (obtained by the application of suitable local gate potentials) play a role of primary importance. It is therefore important to provide a mathematical tool to treat such devices for modelling and simulation purposes.

We start from the consideration that the most interesting quantum effects (also for applications) are concentrated along the heterojunctions, i.e. the interfaces between the different regions of the heterostructure [1,2], while, far from the interface, the dynamics of the carriers is essentially classical. Then, the idea is to extend to graphene the theory of quantum transmission conditions, developed in Refs. [3,4]. Such theory treats the heterojunction as a quantum interface that scatters the carriers according to the laws of Quantum Mechanics, thus providing quantum transmission conditions (QTC) for the drift-diffusion equations that describe the bulk regions. The derivation of QTC exploits the natural connection between the quantum and classical phase-space descriptions of the carrier dynamics provided by the Wigner functions.

In the case of graphene, the Dirac-like nature of the carriers requires a nontrivial extension of the theory, including the electron-hole coupling and the occurrence of a matrix-valued interpolation coefficient [5].

The first numerical experiments [6] show that our framework is able to reproduce some important features of experimental *n-p-n* graphene devices [7], such as the quantum Fabry-Perot-like oscillations of the conductance and their dependence on temperature (Fig. 1).

[1] M. Katsnelson *et al.*, Nat. Phys. 2, 620-625 (2006)

[2] V. Cheianov *et al.*, Science 315, 1252-1255 (2007)

[3] N. Ben Abdallah, J. Stat. Phys. 90, 627-662 (1998)

[4] P. Degond, A. el Ayyadi, J. Comput. Phys. 181, 222-259 (2002)

[5] L. Barletti, C. Negulescu, J. Stat. Phys. 171, 696-726 (2018)

[6] L. Barletti *et al.*, Kinetic Relat. Models 14(3), 407-427 (2021)

[7] A. Young, P. Kim, Nat. Phys. 5, 222-226 (2009)

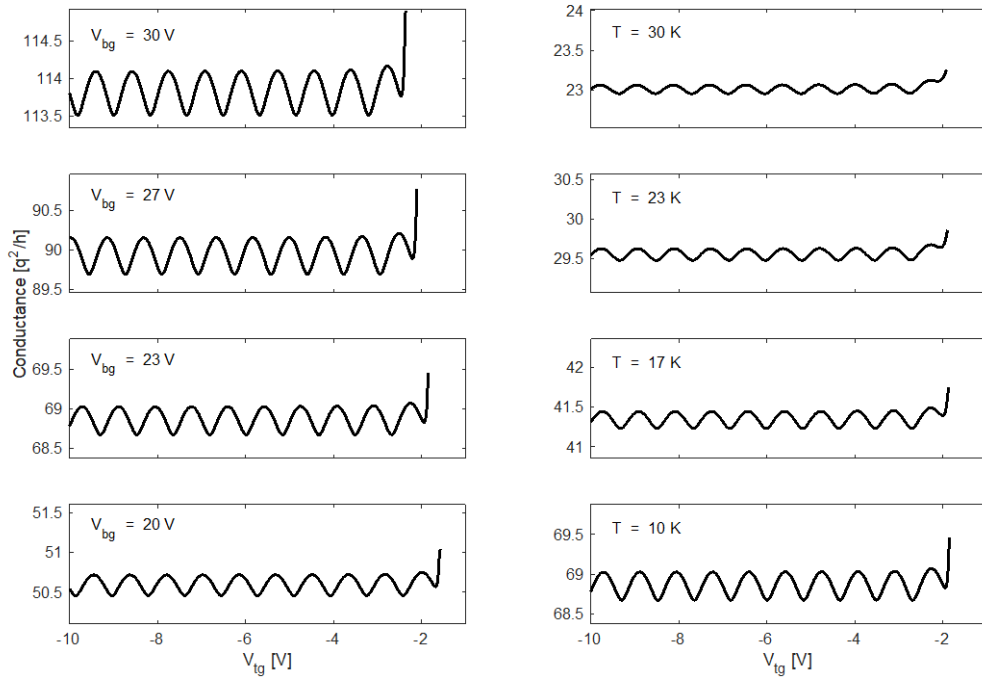


*Fig.1: Simulation of the conductance as a function of the local gate potential  $V_{lg}$  in a n-p-n graphene device for different values of the back-gate potential  $V_{bg}$  and different values of the temperature. The obtained graphs are in good agreement of the experimental results in Ref. [7]. Note, in particular, the conductance oscillations that are due to the Fabry-Perot-like quantum interferences in the region below the local gate. The figure is taken from Ref. [6].*

# Equilibrium Wigner Function for Fermions and Classical Particles

Vito Dario Camiola and Vittorio Romano

*Università degli Studi di Catania*

*Dario.camiola@unict.it*

The continuous process of miniaturization of the electronic devices has led to the investigation of quantum effects in charge transport phenomena. One of the theoretical tools used for such an investigation is the Wigner function [1,2] which, restoring a description in the phase-space, allows an analysis of the transition from the classical to the quantum world which is more intuitive from a physical point of view.

A crucial point is the determination of the Wigner function at equilibrium for many particle systems and here we propose to find such a function as the solution of a Bloch equation for Fermions in the first Brillouin zone. The obtained functions are a modulation of the solution in the non-degenerate case. The figures below show particular solutions calculated around the minima of the energy band by varying temperature ( $\beta = 1/K_B T$ ), Fermi energy and external applied field versus the corresponding classical Boltzmann distribution. The different behavior of classical particles and Fermions are highlighted as discussed in [3].

[1] J. Weinbub, D.K. Ferry, *Appl. Phys. Rev.* 5, 041104 (2018)

[2] L. Luca, V. Romano, *Ann. Phys.* 406, 30-53 (2019)

[3] V.D. Camiola *et al.*, *Entropy* 22, 1023 (2020)

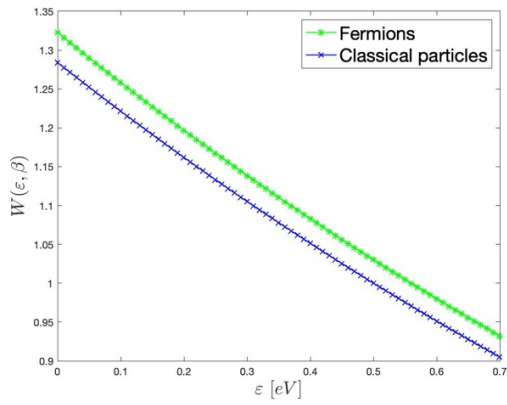


Fig.1: Equilibrium Wigner function (green) and Boltzmann distribution (blue) versus energy (eV) for  $\beta = 0.5$ , external electric field 0.0 eV and Fermi energy 0.5 eV.

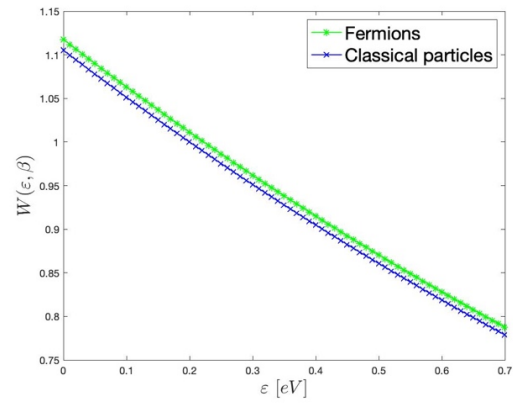


Fig.4: Equilibrium Wigner function (green) and Boltzmann distribution (blue) versus energy (eV) for  $\beta = 0.5$ , external electric field 0.3 eV and Fermi energy 0.5 eV

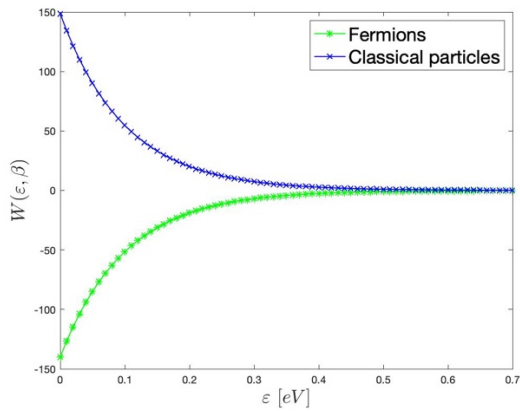


Fig.2: Equilibrium Wigner function (green) and Boltzmann distribution (blue) versus energy (eV) for  $\beta = 10$ , external electric field 0.0 eV and Fermi energy 0.5 eV.

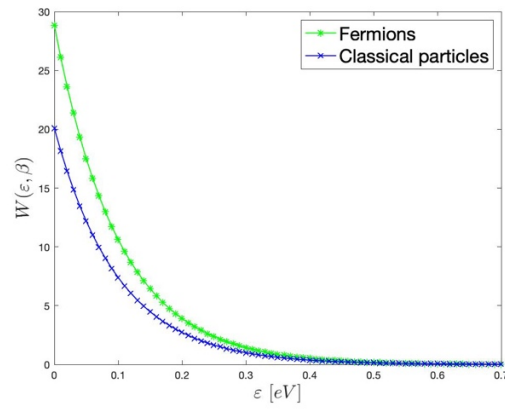


Fig.5: Equilibrium Wigner function (green) and Boltzmann distribution (blue) versus energy (eV) for  $\beta = 10$ , external electric field 0.2 eV and Fermi energy 0.5 eV.

# Application of the Window Function to the Discrete Wigner Transport Equation to Overcome Its Momentum Resolution Limit

Kyoung-Youm Kim<sup>1</sup> and Saehwa Kim<sup>2</sup>

<sup>1</sup>*Department of Electrical Engineering, Sejong University, Seoul 05006, Korea*

<sup>2</sup>*Department of Information and Communications Engineering,  
Hankuk University of Foreign Studies, Gyeonggi-Do 17035, Korea  
kykim@sejong.ac.kr*

The Wigner transport equation (WTE) is a quantum-mechanical counterpart of the classical Boltzmann transport equation (BTE) [1]. Comparing WTE with BTE, we can find a unique term, called the Wigner potential, that performs potential correlation. Quantum effects are incorporated into WTE via the nonlocal characteristics of this correlation term. However, the maximum length of the nonlocal correlation is restricted by the inclusion of classical boundaries. This results in a lower limit on the momentum resolution ( $\Delta_k$ ) of WTE:  $\Delta_k \geq \pi/L$  where  $L$  is the distance between classical boundaries [2]. Considering that  $\Delta_k$  represents the mesh spacing in  $k$  space, we thus cannot pursue a satisfactorily high numerical accuracy in solving the finite-difference-based WTE. If we want to reduce  $\Delta_k$  further, we have to increase  $L$  (if possible). Even if this is possible, the increased  $L$  causes waste of computational resources, increasing the inefficiency of the WTE solver significantly.

In this presentation, we show that the momentum resolution limit (or  $\pi/L$ ) can be overcome by applying a window function [3] to the potential correlation term (see and compare the simulation results in Figs. 1-4). The so-called accuracy balancing problem encountered frequently in the WTE-based device modelling [4,5] can be avoided by using the proposed method.

[1] For a recent review, see J. Weinbub, D. K. Ferry, *Appl. Phys. Rev.* 5, 041104 (2018)

[2] K.-Y. Kim, S. Kim, *Solid-State Electron.* 111, 22 (2015)

[3] A. V. Oppenheim, R. W. Schaffer, *Discrete-Time Signal Processing* (Prentice Hall, 1989)

[4] K.-Y. Kim *et al.*, *J. Comput. Electron.* 16, 148 (2017)

[5] K.-Y. Kim *et al.*, *AIP Adv.* 8, 115105 (2018)

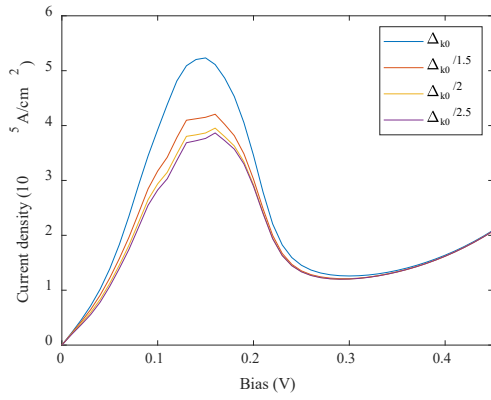


Fig. 1:  $I$ - $V$  characteristics of a resonant tunneling diode (RTD) for  $\Delta_q = 0.25$  nm and  $\Delta_k = \Delta_{k0}$ ,  $\Delta_{k0}/1.5$ ,  $\Delta_{k0}/2$ , and  $\Delta_{k0}/2.5$  where  $\Delta_{k0}$  is the momentum resolution limit ( $\pi/L = 0.021$  nm<sup>-1</sup>). We can find that unphysical results are obtained when  $\Delta_k$  becomes smaller than  $\Delta_{k0}$ .

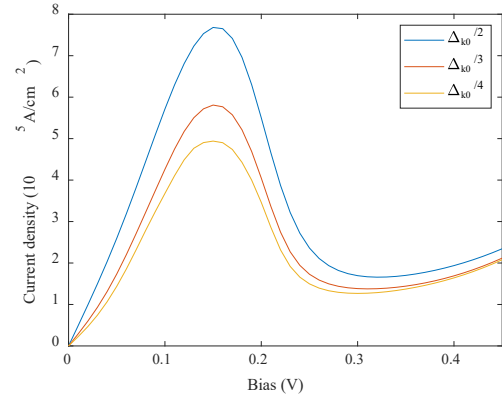


Fig. 3:  $I$ - $V$  characteristics of the same RTD calculated using a "flat top" window function ( $\Delta_q = 0.25$  nm and  $\Delta_k = \Delta_{k0}/2$ ,  $\Delta_{k0}/3$ , and  $\Delta_{k0}/4$ ). We can see that unphysical results do not appear even if  $\Delta_k$  is reduced as small as  $\Delta_{k0}/4$ .

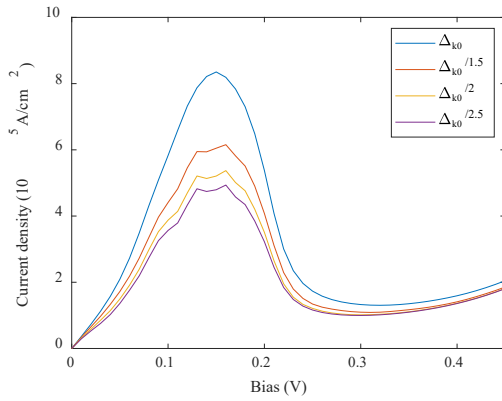


Fig. 2: The same as Fig. 1 for  $\Delta_q = 0.125$  nm.

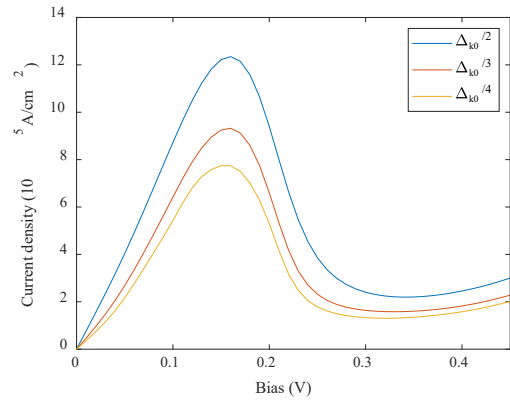


Fig. 4: The same as Fig. 3 for  $\Delta_q = 0.125$  nm.

# Open Boundary Conditions for the Wigner and the Characteristic von Neumann Equation

Robert Kosik, Johann Cervenka, and Hans Kosina  
*Institute for Microelectronics, TU Wien, Austria*  
*kosik@iue.tuwien.ac.at*

Open boundary conditions for the Wigner equation have been introduced by Frensley [1] who used inflow boundary conditions at spatial boundaries. On a coarse mesh Frensley's model produces superficially reasonable solutions, which however are an artifact of numerical diffusion. The model breaks down in the limit of a fine mesh [2].

Frensley's discretization corresponds to anti-periodic boundary conditions in the non-spatial coordinate of the characteristic von Neumann equation. To remedy the breakdown an absorbing imaginary potential can be employed as suggested in [3]. The absorbing potential avoids spurious reflections at non-spatial boundaries in the characteristic equation.

Here we introduce a formulation of open boundary conditions based on a symmetric treatment of spatial and non-spatial coordinates in the characteristic equation. We apply inflow type boundary conditions also at the non-spatial boundaries. For this we use the Fourier transform of the characteristic function in the spatial coordinate which is denoted ambiguity function. We impose the condition that the flow into the domain at non-spatial boundaries is zero.

As shown in Figures 1 and 2 results based on "no inflow" boundary conditions (open BCs) closely reproduce results from the quantum transmitting boundary method (QTBM). In Figure 3 we compare results from open BCs with results when using an absorbing potential and find excellent agreement. This work clarifies the notion of open boundary conditions for the Wigner and the characteristic Neumann equation and demonstrates its numerical robustness.

**Acknowledgements.** This work was partly funded by FWF Austrian Science Fund, project number P33151 "Numerical Constraints for the Wigner and the Sigma Equation".

[1] W. R. Frensley, *Rev. Mod. Phys.* 62(3), 745–791 (1990)

[2] R. Kosik *et al.*, In: *Large-Scale Scientific Computing*, p. 403-410 (Springer, 2020)

[3] L. Schulz, D. Schulz, *IEEE Trans. Nanotechnol.* 18, 830-838 (2019)

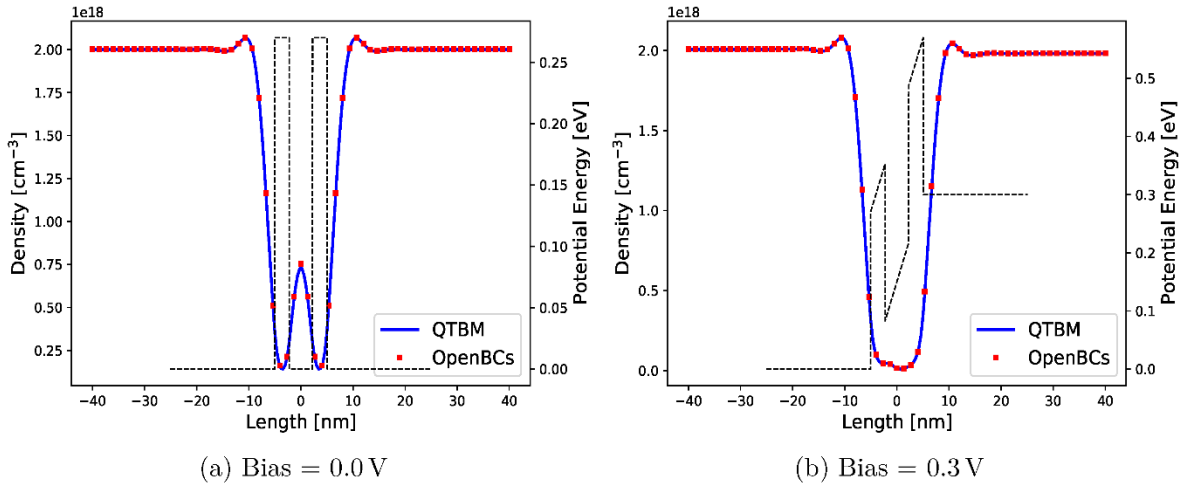


Figure 1: Comparison of the particle density in the active region of a resonant tunneling diode structure for different biases using QTBM and open BCs. The dashed black lines indicate potential energy. The coherence length used is 120 nm. Mesh size  $N_r = 1000$ ,  $N_s = 907$ .

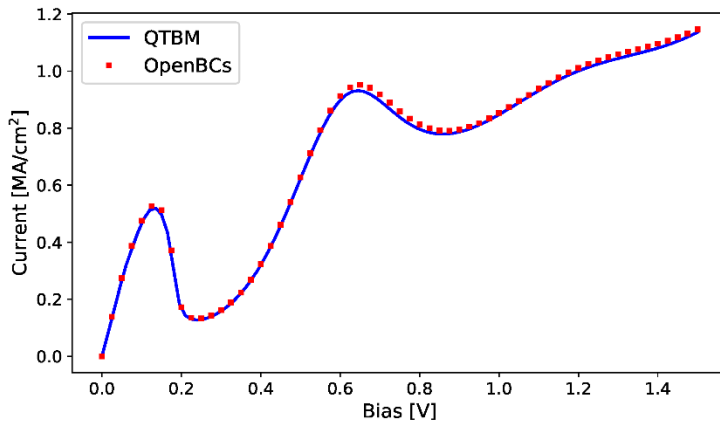


Figure 2: Simulation of the current-voltage curve for the same resonant tunneling structure as used in Fig. 1. Again, good agreement between the solution based on open BCs and the QTBM solution.

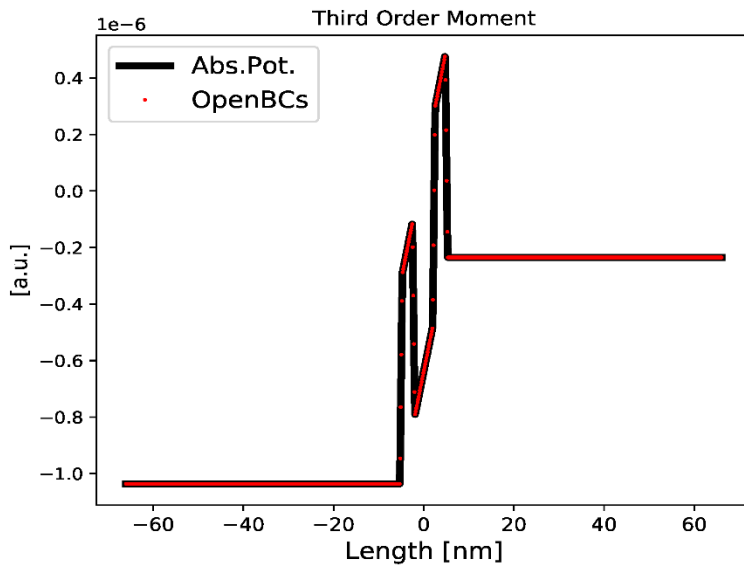


Figure 3: Quality test. The third order moment of the Wigner function (third order derivative of the characteristic function) follows the potential energy. Results from using an absorbing potential (black line) are in excellent agreement with results using open BCs (dotted red). The exact same mesh and the same discrete spatial inflow boundary conditions are used for both simulations (bias 0.3 V, barrier height 0.27 eV).

# Approximation of Multiband Hamiltonians for the Wigner Equation

Lukas Schulz and Dirk Schulz

*Chair for High Frequency Techniques, TU Dortmund, Germany*

*dirk2.schulz@tu-dortmund.de*

For the investigation of devices for THz- and photonic applications, the inherent consideration of intraband tunneling effects as well as interband tunneling effects is of essential importance. For this purpose appropriate Wigner-Transport equations must be available and have to be derived. So far, for the case of intraband tunneling a few approaches have been proposed [1-2], but for the case of interband tunneling appropriate methods are lacking. Two distinct multiband approaches are suitable within the Wigner formalism, namely the two band Kane-model [3] as well as the multiband-envelope function (MEF)-model [4]. The MEF model is preferable due to the direct physical interpretation of the electron and hole wave functions [5]. The latter approach allows a simplification of the formulation of boundary conditions as intermixing states are avoided at the boundaries. As most components are based on heterostructures, the spatially dependent effective mass must also be taken into account.

For the formulation of the Wigner transport equation, it has proven to be useful to start from the von Neumann equation in center mass coordinates and to apply an approach corresponding to the Weyl transformation [6]. This methodology allows the adequate inclusion of the spatially dependent effective mass and multiband models [7, 8]. Furthermore, the CAP method is used to avoid the artifacts that occur with the conventional method [6]. The peculiarity of the numerically approximated transport equation in phase space is that, compared to the conventional equation, which spatially represents a partial differential equation of the first order, a partial differential equation of the second order arises. To formulate the methodology, it is necessary to approximate the differential operators in such a way that the conservation properties, which are reflected in the fulfillment of the continuity equation, are fulfilled. The concept (QLNE) is presented and verified using practical examples.

- [1] H. Kosina, *Int. J. Comput. Eng. Sci.* 2 (2006)
- [2] H. Jiang *et al.*, *J. Comput. Phys.* 229 (2010)
- [3] G. Borgioli *et al.*, *Transp. Theory Stat. Phys.* 32 (2003)
- [4] O. Morandi *et al.*, *Phys. Rev. B* 80 (2009)
- [5] O. Morandi *et al.*, *Phys. Rev. B* 71 (2005)
- [6] L. Schulz *et al.*, *Trans. Nanotechnology* 18 (2019)
- [7] L. Schulz *et al.*, *J. Comput. Electron* 19 (2020)
- [8] L. Schulz *et al.*, *Proc. SISPAD* (2020)

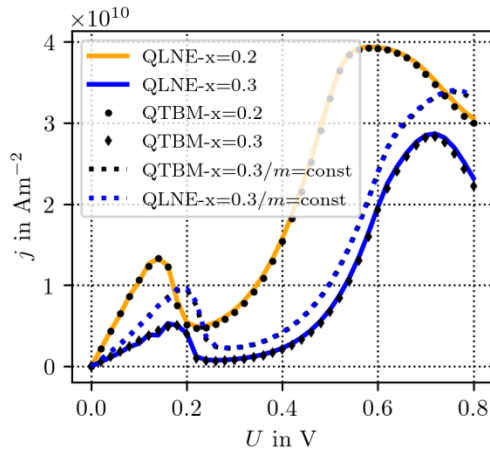


Fig.1a: I-V characteristics for a  $Al_xGa_{1-x}As/GaAs$ -RTD compared with the reference solution from QTBM in the flat-band case. One can observe from Fig. 1a, that without taking into account the spatially dependent effective mass these results differ significantly from those with the spatially dependent effective mass. The results, when compared with the QTBM taking into account the spatially dependent effective mass and intraband tunneling, show a very good agreement.

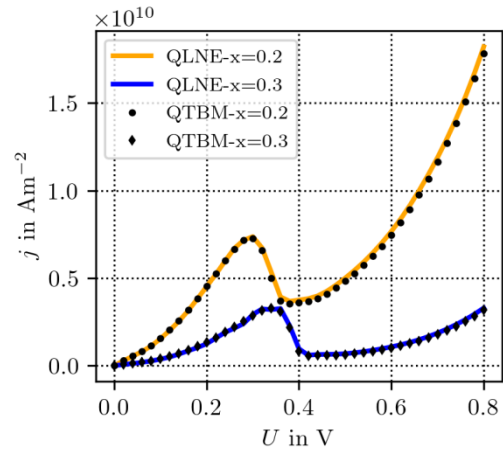


Fig.1b: I-V characteristics for a  $Al_xGa_{1-x}As/GaAs$ -RTD compared with the reference solution from QTBM for the self-consistent case. When comparing the results with the results obtained from the QTBM a very good coincidence can be confirmed.

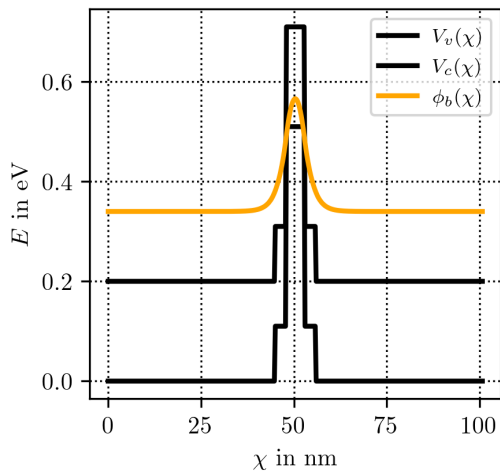


Fig.2a: In another example, a resonant tunnel diode is considered, in which interband tunneling occurs via the coupling between the valence and conduction bands. The valence band diagram is schematically shown. The bounded state relevant for the tunneling process is shown as well.

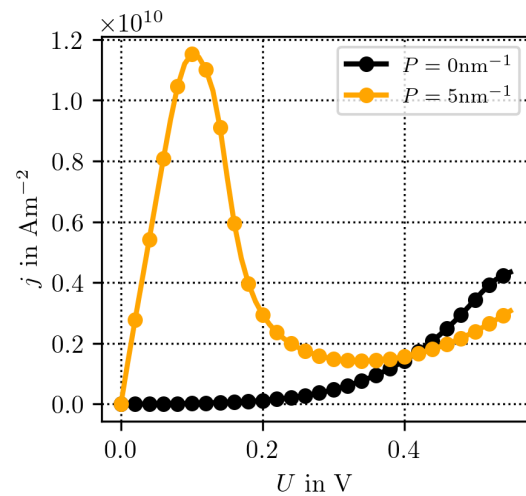


Fig.2b: I-V characteristic with regard to the Kane Parameters  $P$  representing the valence band and conduction band coupling. From the results presented it can be seen that the essential effects of tunneling are considered very well.

# On the Nonphysical Solutions to the Wigner Equation in Electronic Transport Simulation

M. K. Eryilmaz, S. Soleimanikahnoj, and I. Knezevic  
*Department of Electrical and Computer Engineering,  
University of Wisconsin-Madison, Madison, WI 53706, USA*  
*korkmaz2@wisc.edu*

The Wigner transport equation is a useful tool for modeling quantum electronic transport in semiconductors [1,2]. The appeal of the Wigner formalism stems from an intuitive link with semiclassical transport and a straightforward implementation of the common open boundary conditions. However, this boundary scheme has been criticized as incompatible with the nonlocal nature of quantum mechanics, resulting in negative probability densities [3,4].

In this study, we investigate the limits of validity of the standard open boundary condition scheme. We analyze the role of boundary conditions in the behavior of the solutions to the Wigner equation for a finite-sized one-dimensional nanostructure with a potential barrier in the middle and connected to reservoirs of charge. The electrons are simulated as wave packets, with varying packet widths and energies to test the system for nonphysical results.

We show that nonphysical results are related to violation of the Heisenberg uncertainty principle in finite-domain simulations rather than the inflow boundary conditions themselves. By solving the dependent Wigner transport equation, we find that even a valid Wigner function can evolve in time to be unphysical due to an artificial cutoff of coherence at the boundaries. We find that a) as long as boundaries are chosen to be far enough away from strong spatial variations in the device potential and b) the momentum spread of the injected electrons is high enough, the Wigner function remains physical and valid at all times. We provide criteria for what is “far enough” and what constitutes a large enough momentum spread for the injected packets. We show that these conditions do not depend strongly on the form of the device potential and are broadly applicable for Wigner transport simulation.

**Acknowledgements.** This work was supported by DOE (award DE-SC0008712) and UW ECE Splinter Professorship.

- [1] D. Querlioz, P. Dollfus, *The Wigner Monte Carlo Method for Nanoelectronic Devices* (Wiley-ISTE, 2010)
- [2] J. Weinbub, D. K. Ferry, *Appl. Phys. Rev.* 5, 041104 (2018)
- [3] D. Taj *et al.*, *Europhys. Lett.* 74, 1060 (2006)
- [4] R. Rosati *et al.*, *Phys. Rev. B* 88, 035401 (2013)

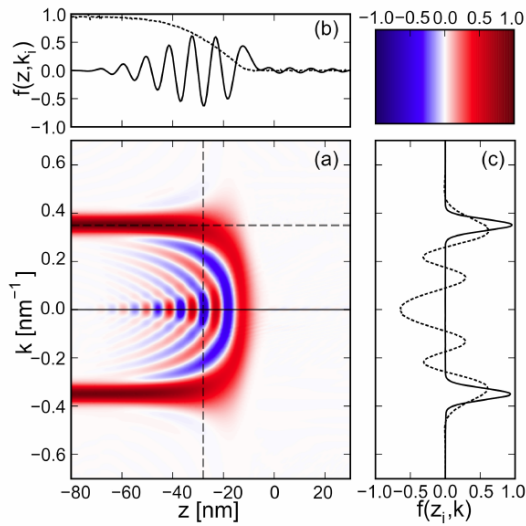


Fig. 1. Steady-state Wigner function for a cosine barrier potential and incident electron momentum spread given by  $\lambda = 30$  nm (small  $\lambda$  indicates large momentum spread). (a) Phase-space map where red (blue) represents positive (negative) values of the Wigner function. (b) Constant- $k$  slices for  $k=0$  (solid) and  $0.35$  nm<sup>-1</sup> (dashed). (c) Constant- $z$  slices for  $z = -80$  nm (solid) and  $z = -28$  nm (dashed).

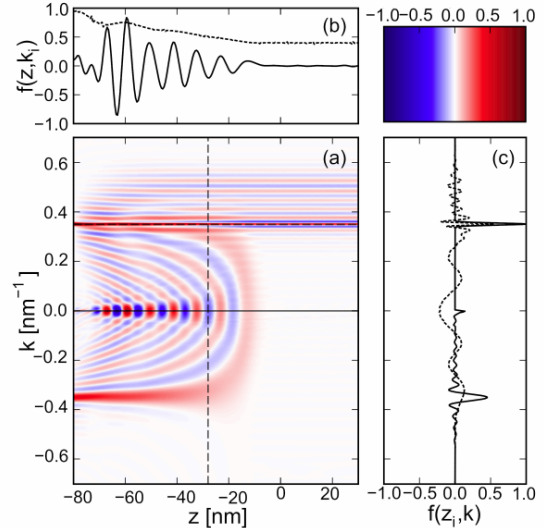


Fig. 2. Steady-state Wigner function for a cosine barrier potential and incident electron momentum spread given by  $\lambda = 200$  nm (large  $\lambda$  indicates small momentum spread). (a) Phase-space map where red (blue) represents positive (negative) values of the Wigner function. (b) Constant- $k$  slices for  $k=0$  (solid) and  $0.35$  nm<sup>-1</sup> (dashed). (c) Constant- $z$  slices for  $z = -80$  nm (solid) and  $z = -28$  nm (dashed). Note the spurious interference features.

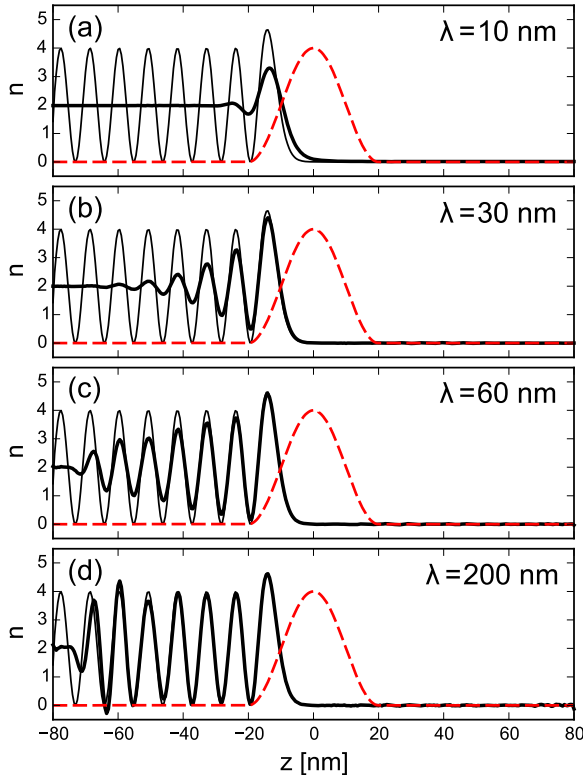


Fig. 3. Steady-state probability densities (thick solid black curves) for different values of the wave spread  $\lambda$ , keeping the system length constant at 160 nm. Dashed red curves show the device potential in arbitrary units. Also shown is the probability density obtained from plane-wave calculations (thin solid black curves). When  $\lambda$  is so large (momentum spread so small) that the interference pattern extends all the way to the contact area, the probability density near the left contact may exhibit unphysical negative values, as it does in (d).

# On the Wigner-Boltzmann Equation of Motion for Scenarios with Non-Commuting Energy Momentum Operators

Matteo Villani and Xavier Oriols

*Universitat Autònoma de Barcelona, Bellaterra, Barcelona, Spain*

*Matteo.Villani@uab.cat*

The equation of motion for the Wigner function applied to the simulation of electron nanodevices requires, apart from a coherent term, needs an additional collision term to describe the interaction of the open system with the environment [1]. The exact shape of this collision term is unknown and reasonable approximations are needed. For flat potential conditions, the exchange of a momentum  $\lambda$  between an initial  $\psi_i(x, t)$  and a final  $\psi_f(x, t)$  wave packets is given by  $\psi_f(x, t) = e^{i\lambda x/\hbar}\psi_i(x, t)$  which is translated into the Wigner representation as a transition between two phase-space points (or regions) with identical positions and different momenta (see Fig. 1). This observation has been used to justify the use of the Boltzmann collision operator into the Wigner-Weyl transform of the Liouville equation (i.e., the so-called Wigner-Boltzmann equation of motion [2,3]).

In this conference, we discuss on the application of the Wigner-Boltzmann equation of motion in scenarios with an arbitrary potential, where the energy and momentum operators do not commute: a well-defined change of momentum do not correspond to a well-defined change of energy (and vice-versa). We consider two scattering models: Model A where the mean energy of the final wave packet is increases/decreased with respect to the initial one, and Model B where the mean momentum is changed (which corresponds to the mentioned implementation of the Boltzmann collision operator in phase-space). We study a spontaneous emission in a double barrier structure, where an electron in the second resonant level loses energy and reaches the first level. With Model A, the initial zero probability of the second level in the middle of the well in Fig. 2 disappears in Fig. 3 when the electron occupies the first level. On the contrary, Model B does not produce the desired state transition and the phase-space distribution typical of the second level is still present in Fig. 4. This unphysical feature of Model B is also seen in Fig. 6 where the expected decrease of the energy of the electron (due to the emission of a photon) is not observed. We conclude that the implementation of the Boltzmann collision operator is valid for flat (or quasi-flat) potentials, but not for arbitrary ones where the momentum and energy operators do not commute and a change in energy is not equivalent to a change in momentum. Model B can lead to artificial oscillatory behavior, which can lead to relevant mistakes when discussing high frequency electronics in double barrier structures [4].

[1] J. Weinbub *et al.*, Appl Phys. Rev. 5, 041104 (2018)

[2] Z. Zhan *et al.*, J. Comput. Electron. 15, 1206-1218 (2016)

[3] E. Colomes *et al.*, J. Comput. Electron. 14, 894 (2015)

[4] M. Villani *et al.*, Electron. Dev. Lett. 42, 224-227 (2021)

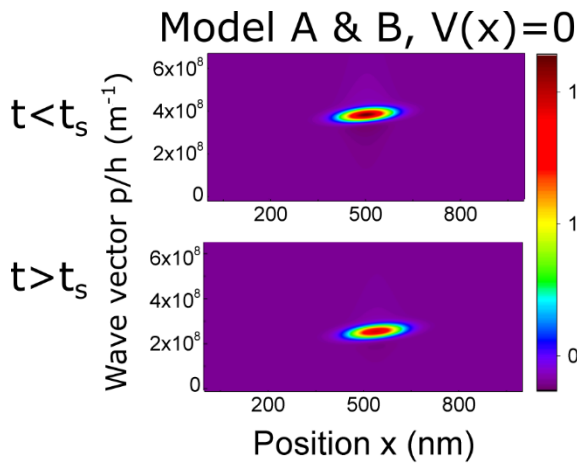


Fig.1: Transition of the Wigner function from a state of mean energy  $0.12\text{eV}$  (momentum  $3.59 \cdot 10^8 \text{ m}^{-1}$ ), to mean energy  $0.03\text{eV}$  (momentum  $1.79 \cdot 10^8 \text{ m}^{-1}$ ), in flat potential conditions.

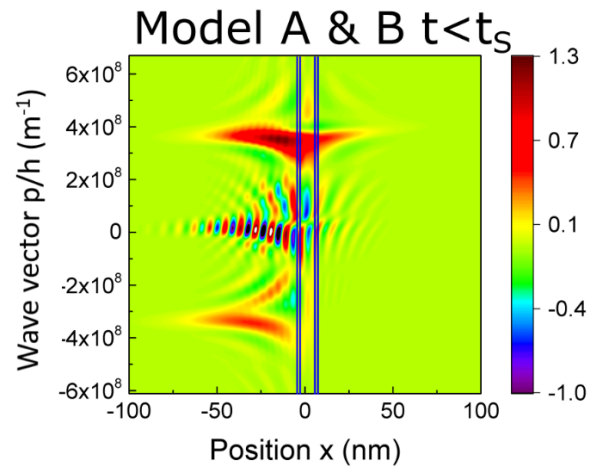


Fig.2: Wigner function for an electron in the second resonant level of a double barrier before (scattering) spontaneous emission.

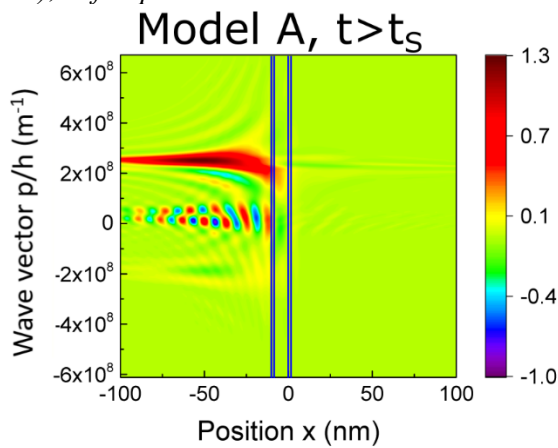


Fig.3: Wigner function interacting with a double barrier, after spontaneous emission (Model A). The electron “jumps” from the second to the first resonant level.

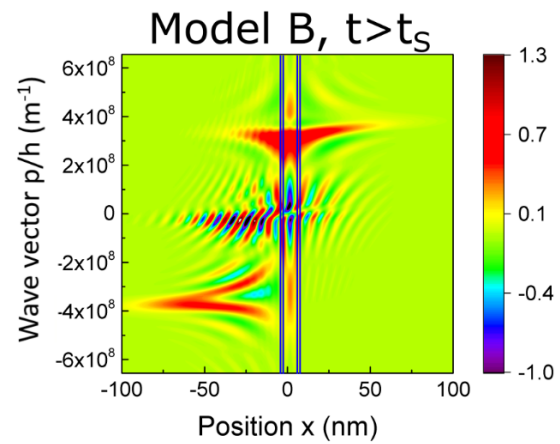


Fig.4: Wigner function interacting with a double barrier, after spontaneous emission (Model B). The electron remains in the second resonant level.

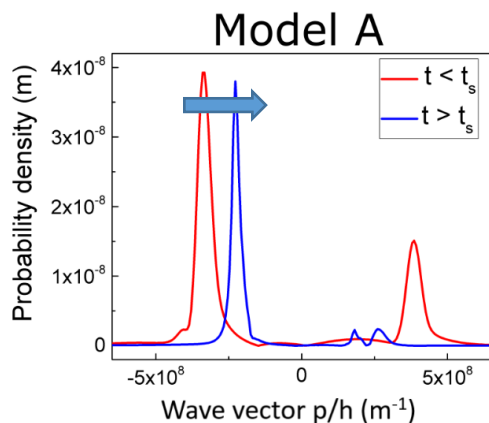


Fig.5: Evolution of the momentum components of the Wigner function in Fig. 2 and in Fig 3. Red line refers to the probability density before, blue line after the scattering.

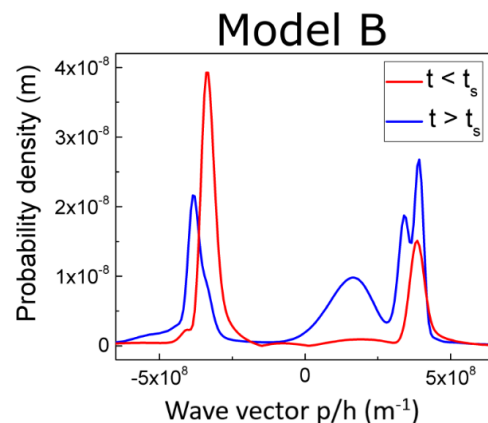


Fig.6: Evolution of the momentum components of the Wigner function in Fig. 2 and in Fig. 4. Red line refers to the probability density before, blue line after the scattering.

# Processing Quantum Signals Carried by Electrical Currents

Benjamin Roussel<sup>1</sup>, Clément Cabart<sup>3</sup>, Gwendal Fève<sup>2</sup>, and Pascal Degiovanni<sup>3</sup>

<sup>1</sup>*Department of Applied Physics, Aalto University, 00076 Aalto, Finland*

<sup>2</sup>*Laboratoire de Physique de l'École Normale Supérieure, ENS, Université PSL, CNRS, Sorbonne Université, Université de Paris, F-75005 Paris, France*

<sup>3</sup>*Univ Lyon, ENS de Lyon, Université Claude Bernard Lyon 1, CNRS, Laboratoire de Physique, F-69342 Lyon, France*  
*Pascal.Degiovanni@ens-lyon.fr*

The recent developments in the coherent manipulation of electrons in ballistic conductors have led to the generation of time-periodic quantum electrical currents carrying one to few excitations per period. This has opened the way to the demonstration of several « electron quantum optics » experiments analogous to famous experiments performed with photons [1]. These quantum electrical currents can be envisioned as carrier of quantum information for applications in quantum technologies. But in this perspective, we need to be able to visualize their single particle content, a task for which the electronic Wigner distribution function appears to be very well suited [2]. A first step towards understanding how quantum information is encoded within these quantum electrical currents is then to describe their single particle content in the simplest way.

In this talk, I will present such a description for periodic quantum electrical currents in terms of elementary electron and hole excitations, together with their emission probabilities and coherences [3]. This electron quantum optics analogue of the Kármán Loève decomposition for classical signals therefore provides us with the electronic analogue of music notes and musical score at the single electron level (see Fig. 1). This procedure has recently been applied to the tomographic reconstruction of the single electron coherence in an experiment, therefore leading to the first quantitative analysis of its single particle content [4].

[1] E. Bocquillon *et al.*, *Ann. Phys. (Berlin)* 526, 1-30 (2014)

[2] D. Ferraro *et al.*, *Phys. Rev. B* 88, 205303 (2013)

[3] B. Roussel *et al.*, *Phys. Rev. X Quantum* 2, 020314 (2021)

[4] R. Bisognin *et al.*, *Nature Commun.* 10, 3379 (2019)

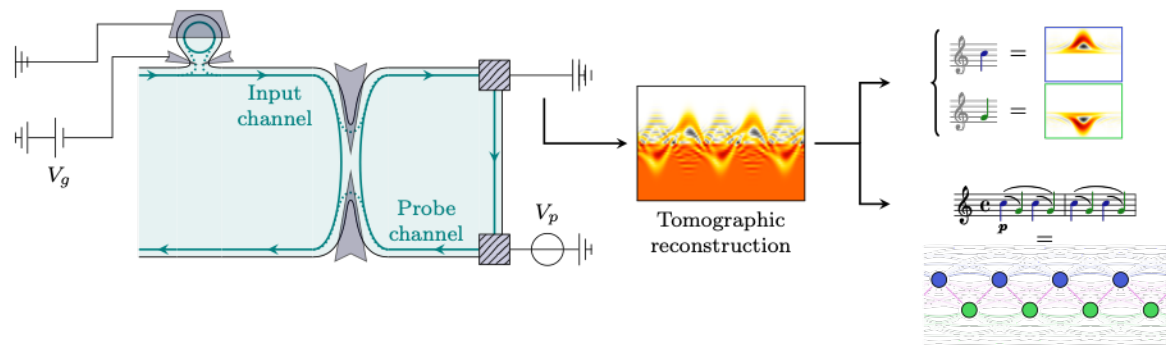


*Fig.1: Extracting the single particle content from a quantum electrical current. Left part: the Hong–Ou–Mandel interferometer uses two-particle interferences to encode the overlap between the injected single electron coherences into the measurable signal (outgoing current noise). Middle part: the Wigner representation of the reconstructed single electron coherence. Right part: decomposition of single electron coherence in terms of electronic atoms of signal (analogues to musical notes) arranged according to a “quantum coherence score” (analogue of the music score).*

# Quantum Corrected Hydrodynamical Models for Charge Transport Based on the Equilibrium Wigner Function

Vito Dario Camiola and Vittorio Romano

*Università degli Studi di Catania*

*romano@dmf.unict.it*

Nanoscale semiconductor devices are playing an increasingly important role in advanced microelectronic applications, including multiple-state logic and memory devices. Therefore, in modeling and simulations of semiconductor devices of ultra-small size under strong electric fields, quantum mechanical effects have to be taken into account. Graphene, consisting of an isolated single atomic layer of graphite, is an ideal candidate for ultimate scaled electron devices.

To take into account quantum phenomena, the semiclassical Boltzmann equation is not enough to describe charge transport. As a starting point for deriving the quantum corrections to the semiclassical model, we consider the Wigner equation (see [1] for a review about its use in the applications). At zero order we recover the semiclassical models obtained by exploiting the Maximum Entropy Principle (MEP) [2]. Second order corrections are obtained from the scaling of high field and collision dominated regime. In the limit of high collisional frequency of the quantum correction to the collision operator, this is equivalent to determine the equilibrium Wigner function. This latter is obtained solving the corresponding Bloch equation [3,4].

Explicit expressions for the quantum correction in the MEP hydrodynamic model are written [4]. The numerics is rather involved and is currently under investigation by the authors.

[1] J. Weinbub, D.K. Ferry, *Appl. Phys. Rev.* 5, 041104 (2018)

[2] V. D. Camiola *et al.*, *Charge Transport in Low Dimensional Structures: The Maximum Entropy Approach* (Springer, 2020)

[3] L. Luca, V. Romano, *Ann. Phys.* 406, 30-53 (2019)

[4] V. D. Camiola *et al.*, *Entropy* 22, 1023 (2020)



# Quantum-State Verification in Phase Space

Russell P. Rundle

*School of Mathematics, Fry Building, University of Bristol, UK*

*r.rundle@bristol.ac.uk*

The Wigner function is a valuable tool in understanding certain properties of a quantum state, whether capturing non-local correlations that manifest with negative quasiprobabilities or getting a sense of the level of coherence of a state. Further, the Wigner function has been used as a method of state verification, where in Ref. [1] we used such a method to verify the construction of a five-qubit GHZ state using IBM's qx, which can be seen in Fig. [1]. Such methods can be very powerful in a qualitative sense, where verification of certain properties is desirable, such as characteristics of entanglement and coherence.

Here, as well as these qualitative results, we will discuss the possible quantitative approaches one can take in state verification through the lens of phase-space methods. We will show how this can be done not only by using the Wigner function, but also its Fourier transform – the Weyl characteristic function – and the associated Q and P functions.

We will provide the framework from Ref. [2] with which one can generate an informationally complete function in phase space, as well as results from Ref. [3] where we equate the Wootters formulation of the Wigner function with the Stratonovich formulation, as is shown in Fig. [2], where the points on each sphere correspond to elements of the Wootters formulation. With this framework we will then discuss the structure of symmetric informational completeness in the Wigner function and provide an overview of quantum-state verification in phase space.

[1] R. P. Rundle *et al.*, Phys. Rev. A 96, 022117 (2017)

[2] R. P. Rundle *et al.*, Phys. Rev. A 99, 012115 (2019)

[3] R. P. Rundle, M. J. Everitt, Adv. Quant. Technol., 2100016 (2021)

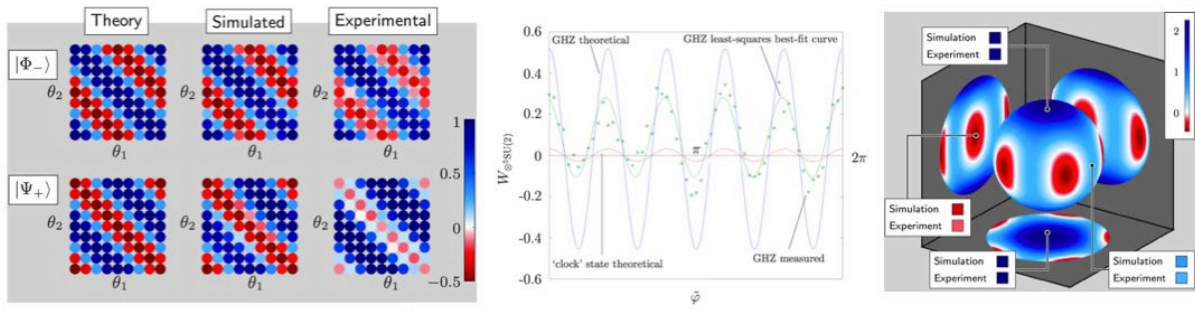


Fig. 1: From [1] shows experimental results from IBM qx, taking direct measurements of the Wigner function of maximally entangled states.

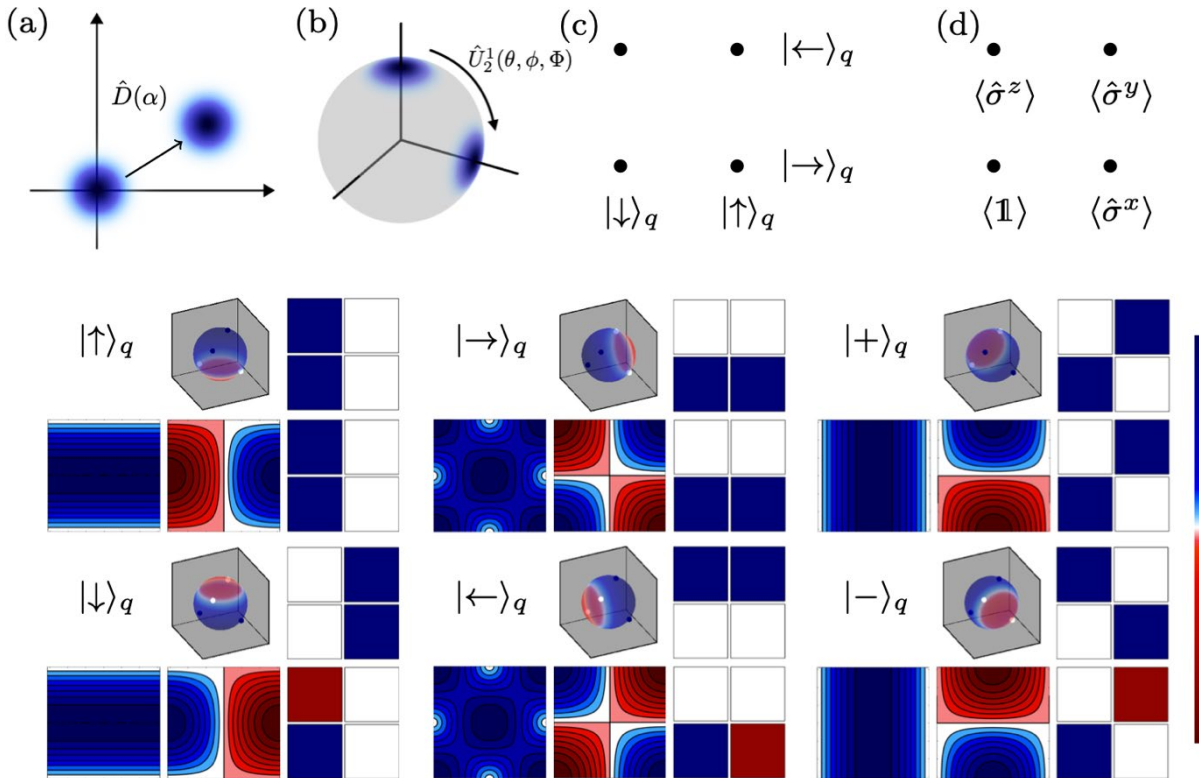


Fig. 2: From [2]. (a)-(d) show the structure of the phase space for (a) the Heisenberg Weyl group, (b) qubit  $SU(2)$  spin-1/2, (c) qubit toroidal lattice, (d) discrete Weyl function. We then show the equivalence between the discrete Wootters formulation and the continuous Stratonovich formulation of the Wigner function for qubits, where the points on the spheres are the corresponding points of the Wootters function create a tetrahedron on the Bloch sphere. For each state we show (left-to-right, top-to-bottom) the state, the Stratonovich Wigner function for the state, the corresponding Wootters Wigner function, the real value of the continuous Weyl function, the imaginary value for the continuous Weyl function and the discrete Weyl function.

# Hybrid Quantum-Classical Mechanics: Lessons from Wigner

Mustafa Amin and Mark Walton

*University of Lethbridge, Lethbridge, Alberta, Canada*

*m.amin@uleth.ca*

A consistent theory of interacting quantum and classical systems is desirable for multiple reasons. For systems where some degrees of freedom are treated quantum mechanically and others, classically (such as electrons and nuclei) the quantum back-reaction on the classical could be of importance. Having a quantum-classical theory is computationally less demanding than a full quantum description while offering microscopic details that are not captured by more familiar semiclassical approximations.

Despite multiple efforts, such as the dynamical brackets introduced by Aleksandrov [1], Boucher and Traschen [2], Anderson [3] and others, hybrid constructions have been shown to be inconsistent in various no-go theorems (see [4], e.g.). If one desires to couple classical and quantum variables in a way that goes beyond mere approximation, then these no-go theorems show that hybrid dynamics does not, in general, preserve important quantities such as canonical commutation relations.

Analysing the problem from Wigner-inspired approaches to quantum mechanics in phase space, we were able to pinpoint the exact origin of this inconsistency [5]. This allows us to have concrete grounds on which we can find ways around these no-go theorems. Specifically, we show that pure quantum or pure classical dynamical variables can, indeed, consistently interact with one another, while the problem lies when one tries to study hybrid dynamical variables. Moreover, we show that a certain class of classical variables can be combined with quantum ones to form hybrid variables that do obey the desired consistency conditions.

[1] I. V. Aleksandrov, *Z. Naturforsch. A* 36, 902 (1981)

[2] W. Boucher, J. Traschen, *Phys. Rev. D* 37, 3522 (1988)

[3] A. Anderson, *Phys. Rev. Lett.* 74, 621 (1995)

[4] V. Gil, L. L. Salcedo, *Phys. Rev. A* 95, 012137 (2017)

[5] M. Amin, M. Walton, arXiv:2009.09573 (2020)

# Coherent Subspaces in a Hilbert Space with Prime Dimension and Q Functions

Apostolos Vourdas

*Department of Computer Science, University of Bradford, UK*

*avourdas@bradford.ac.uk*

Coherent subspaces spanned by a finite number of coherent states are introduced, in a quantum system with Hilbert space that has odd prime dimension  $d$ . The set of all coherent subspaces is partitioned into equivalence classes, with  $d^2$  subspaces in each class. The corresponding coherent projectors within an equivalence class, have the 'closure under displacements property' and also resolve the identity. Different equivalence classes provide different granularisation of the Hilbert space, and they form a partial order 'coarser' (and 'finer'). In the case of a two-dimensional coherent subspace spanned by two coherent states, the corresponding projector (of rank 2) is different than the sum of the two projectors to the subspaces related to each of the two coherent states. We quantify this with 'non-additivity operators' which are a measure of quantum interference in phase space, and also of the non-commutativity of the projectors. Generalized Q and P functions of density matrices, which are based on coherent projectors in a given equivalence class, are introduced. A corresponding Wigner function will also be defined. Analogues of the Lorenz values and the Gini index (which are popular quantities in Mathematical Economics) are used here to quantify the inequality in the distribution of the Q function of a quantum state, within the granular structure of the Hilbert space. Various examples demonstrate these ideas.

[1] A.Vourdas, J. Phys. A53, 215201 (2020)

# Wigner-Function Applications in Magnetic-Confinement Fusion: Propagation of High-Frequency Beams and Evolution of Geodesic-Acoustic Packets

Emanuele Poli<sup>1</sup>, Alberto Bottino<sup>1</sup>, Omar Maj<sup>1</sup>

Francesco Palermo<sup>1,2</sup>, and Hannes Weber<sup>1</sup>

<sup>1</sup>*Max-Planck-Institut für Plasmaphysik, Garching bei München, Germany*

<sup>2</sup>*Culham Centre for Fusion Energy, Abingdon, UK*

*emanuele.poli@ipp.mpg.de*

The goal of this contribution is to discuss selected non-quantum applications of Wigner-function techniques in magnetically confined fusion plasmas. The first example is the propagation of electromagnetic mm-wave beams through anisotropic media including random density fluctuations of arbitrary spatial scale, whose amplitude satisfies the Born approximation [1]. A direct solution of the relevant steady state wave kinetic equation (WKE) employing a ray-based Monte Carlo method has been developed recently [2, Fig. 1,2], while ongoing work focuses on a paraxial solution of the WKE with the aim to reduce the associated computational effort [3]. The focus of this contribution is on an axisymmetric, one-dimensional plasma oscillation occurring in toroidal plasmas as localized radial packets, called geodesic acoustic mode (GAM). The problem is tackled with a paraxial Wigner-function approach that includes the treatment of damping, following a related work in non-Hermitian quantum mechanics [4]. Analytic solutions obtained in the linear, homogeneous-plasma limit agree very well with the results of (physically mode comprehensive) gyrokinetic particle-in-cell simulations. A broadening of the packet due to the stronger damping of higher wavenumbers is found, which can compete with the dispersive broadening [5, Fig. 3,4]. Nonlinear oscillations (without linear damping) are shown to obey a nonlinear Schrödinger equation. The possibility of Landau damping due to the nonlinearity, as it follows from a Wigner-function approach for partially coherent packets [6], is discussed. Finally, the treatment of the interplay between short and long scales in plasma turbulence employing a wave-kinetic approach [see e.g. 7] is briefly addressed.

[1] S. W. McDonald, Phys. Rev. A 43, 4484 (1991)

[2] H. Weber *et al.*, EPJ Web of Conf. 87, 01002 (2015)

[3] Electromagnetic wave beam applications are discussed in more detail by H. Weber in this workshop.

[4] E.-M. Graefe, R. Schubert, Phys. Rev. A 83, 060101 (2011)

[5] E. Poli *et al.*, Phys. Plasmas 27, 082505 (2020)

[6] B. Hall *et al.*, Phys. Rev. E 65, 035602 (2002)

[7] D. E. Ruiz *et al.*, J. Plasma Phys. 85, 905850101 (2019)

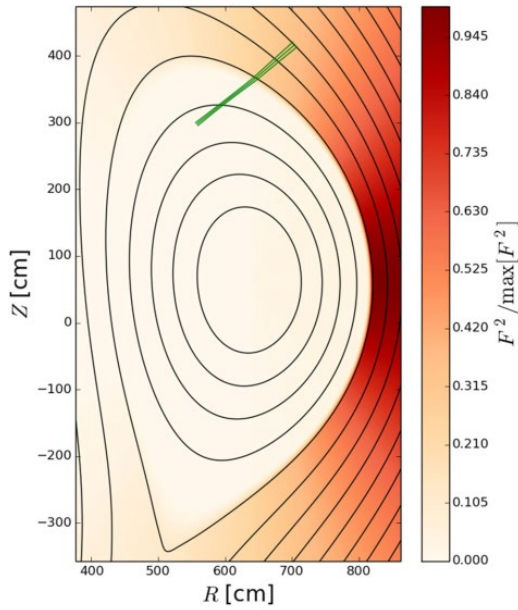


Fig.1: Propagation of a 170 GHz electromagnetic beam (in green) through a vertical cross section of an ITER plasma [A. Snicker et al., Nucl. Fusion **58**, 016002 (2018)]. The confined plasma is shown by closed black contours. The density fluctuations (red scale) are mainly localized just outside the confined plasma.

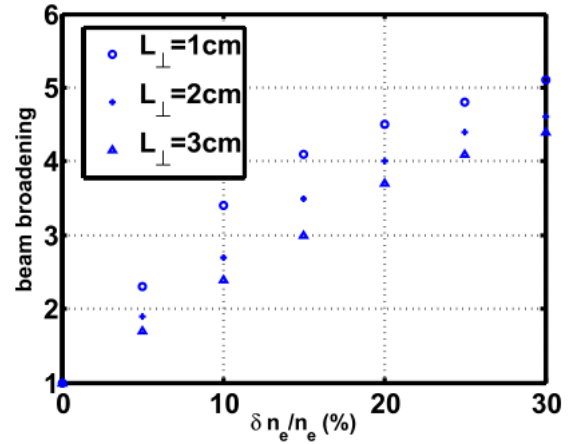


Fig.2: Broadening of the power-absorption profile with respect to the fluctuation-free case for a predicted ITER plasma scenario as a function of the fluctuation level [A. Snicker et al., Nucl. Fusion **58**, 016002 (2018)]. Large broadening can impair some of the foreseen applications of mm-wave beams in tokamak reactors.

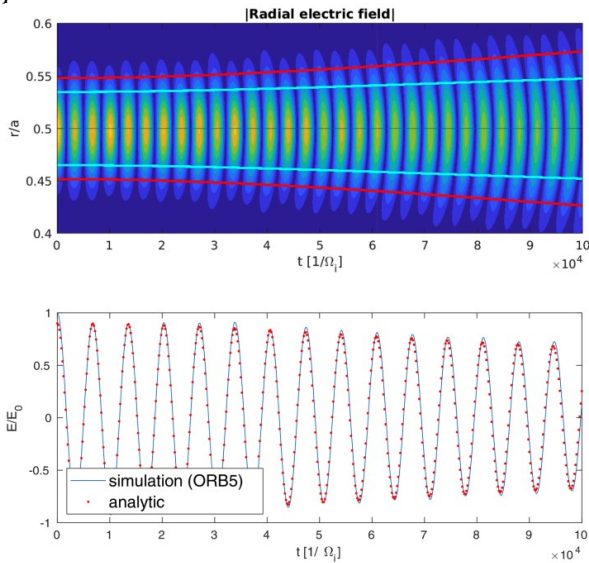


Fig.3: Linear evolution of the absolute value of the GAM electric field (x-axis: time in cyclotron units; y-axis: radial coordinate normalized to the plasma radius) for a case without damping, showing the diffusive broadening of the packet (upper panel). Time evolution of the electric-field amplitude at the centre of the packet. The amplitude decrease ensures energy conservation as the packet broadens [5]. The agreement between the analytically predicted evolution and the results of PIC simulations is very good (lower panel).

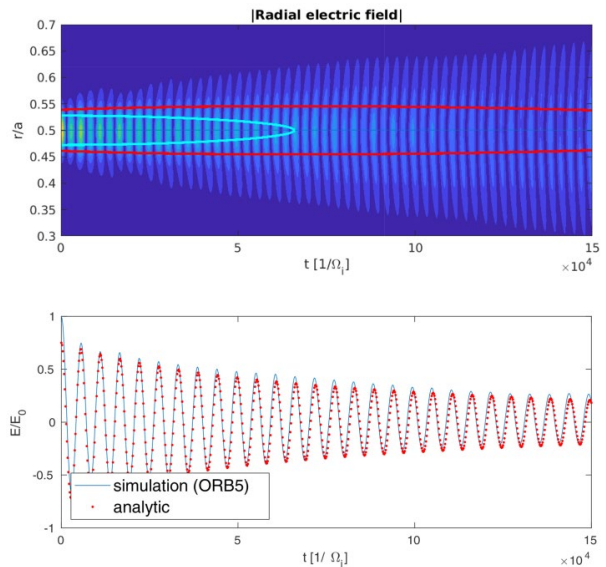


Fig.4: Same as Fig. 3 for a case with significant (Landau) damping. Again, the agreement between analytic theory and simulations is remarkably good.

## Wigner Dynamics with Spin Effects

Giovanni Manfredi<sup>1</sup>, Nicolas Crouseilles<sup>2</sup>, Yingzhe Li<sup>2</sup>, and Paul-Antoine Hervieux<sup>1</sup>

<sup>1</sup>*Université de Strasbourg, CNRS, Institut de Physique et Chimie des Matériaux, France*

<sup>2</sup>*Université de Rennes, INRIA, France*

*giovanni.manfredi@ipcms.unistra.fr*

Dense plasmas, with densities approaching or exceeding  $10^{28} \text{ m}^{-3}$ , are routinely encountered in metallic nanostructures, compact astrophysical objects such as neutron stars, and laser-plasma experiments. At those densities, quantum effects are expected to play some important role. To investigate such quantum plasma dynamics, Wigner function methods constitute a tool of choice. Most early works disregarded the electron spin, which is a fundamental quantum effect in many experiments involving magnetic nanostructures [1].

Simulations of spin-dependent quantum plasmas are computationally complex, as the corresponding Wigner distribution is not a scalar quantity, but a  $2 \times 2$  matrix [2–4]. However, it is possible to define an equivalent scalar distribution that evolves in an extended 8D phase space [5], where the spin is treated as a classical variable defined by two angles on the unit sphere.

We derived a semiclassical Wigner equation with spin effects by expanding the full quantum model to first order in the Planck constant. In this “spin-Wigner” (or spin-Vlasov) model, the mechanical motion of the electrons is classical, while the spin dynamics is fully quantum [4]. We have used the extended phase-space formalism to construct a particle-in-cell (PIC) code that solves the self-consistent spin-Vlasov-Maxwell equations. The numerical scheme is based on a geometric Hamiltonian representation of the full system of equations [6, 7].

As an example of application, we study the impact of spin effects on the interaction of an intense laser source with a dense plasma, focusing in particular on the stimulated Raman scattering (SRS). SRS is a parametric instability whereby an incident electromagnetic wave drives a scattered electromagnetic wave and an electron plasma wave. Here, we investigate how SRS is modified by spin effects and how the spin polarization is destroyed by the onset of the instability.

[1] J.-Y. Bigot *et al.*, *Nature Phys.* 5, 515–520 (2009)

[2] J. Hurst *et al.*, *Eur. Phys. J. D* 68, 176 (2014)

[3] J. Hurst *et al.*, *Phil. Trans. Royal Soc. A* 375 (2092), 20160199 (2017)

[4] G. Manfredi *et al.*, *Rev. Mod. Plasma Phys.* 3, 1-55 (2019)

[5] J. Zamanian *et al.*, *New J. Phys.* 12, 43019 (2010)

[6] M. Marklund, P. J. Morrison, *Phys. Lett. A* 375, 2362 (2011)

[7] Y. Li *et al.*, *J. Comput. Phys.* 405, 109172 (2020)

## Distinguishing Quantum Features in Classical Propagation

Kelvin Titimbo<sup>1,2</sup>, Gabriel M. Lando<sup>2</sup>, and Alfredo M. Ozorio de Almeida<sup>2</sup>  
<sup>1</sup>*CAS Key Laboratory of Theoretical Physics, Institute of Theoretical Physics,  
Chinese Academy of Sciences, Beijing 100190, China*  
<sup>2</sup>*Centro Brasileiro de Pesquisas Físicas,  
Rua Xavier Sigaud 150, 22290-180, Rio de Janeiro, R. J., Brazil*  
*alfredozorio@gmail.com*

The strictly classical propagation of an initial Wigner function, referred to as TWA or LSC-IVR, is considered to provide approximate averages, despite not being a true Wigner function: it does not represent a positive operator. We here show that its symplectic Fourier transform, the truncated chord approximation (TCA), coincides with the full semiclassical approximation to the evolved quantum characteristic function (or chord function) in a narrow neighbourhood of the origin of the dual chord phase space. Surprisingly, this small region accounts for purely quantum features, such as blind spots and local wave function correlations, as well as the expectation of observables with a close classical correspondence. Direct numerical comparison of the TCA with exact quantum results verifies the semiclassical predictions for an initial coherent state evolving under the Kerr Hamiltonian. The resulting clear criterion for any further features, which may be estimated by classical propagation, is that, within the chord representation, they are concentrated near the origin.

[1] K. Titimbo *et al.*, Phys. Scr. 96, 015219 (2021)

# Wigner-Function-Based Solution Schemes for Electromagnetic Wave Beams in Fluctuating Media

Hannes Weber, Omar Maj, and Emanuele Poli  
*Max Planck Institut für Plasmaphysik, Boltzmannstraße 2,  
D-85748 Garching bei München, Germany  
hannes.weber@alumni.uni-ulm.de*

Electromagnetic waves are described by Maxwell's equations together with the constitutive equation of the considered medium. The latter equation in general may introduce complicated operators. As an example, for electron cyclotron (EC) waves in a hot plasma, an integral operator is present [1]. Moreover, the wavelength and computational domain may differ by orders of magnitude making a direct numerical solution unfeasible.

On the other hand, given the free-space wavelength  $\lambda_0$  and the scale  $L$  of the medium inhomogeneity, an asymptotic solution for a wave beam can be constructed in the limit  $\kappa=2\pi L/\lambda_0 \rightarrow \infty$ , referred to as the semiclassical limit. Such procedure allows one to compute efficiently the high-frequency oscillations and the beam shape which is localized around a central ray, cf. the paraxial Wentzel-Kramer-Brillouin (pWKB) approximation [2].

However, the semiclassical limit of the wave field may be inaccurate when random short-scale fluctuations of the medium are present. A phase-space description based on the statistically averaged Wigner function may solve this problem. The Wigner function in the semiclassical limit is described by the wave kinetic equation (WKE), derived from the Maxwell's equations [3].

We present several solution strategies for the WKE. (i) A direct numerical solution is obtained from the Monte-Carlo ray tracing code WKBeam [4]. (ii) A paraxial expansion of the Wigner function around the central ray provides a set of ordinary differential equations (phase-space beam tracing equations), for the Gaussian beam width along the central ray trajectory [Fig.1]. (iii) Nonetheless, the assumption of a Gaussian beam cross section is appropriate only when the effect of random fluctuations can be described as a diffusion process. For the general case, we show numerical experiments that support the validity of a superposition of Gaussians, referred to as multi-Gaussian ansatz [Fig.2].

[1] E. Westerhof, *Trans. Fusion Sci. Technol.* 49, 87 (2011)

[2] G. V. Pereverzev, *Rev. Plasma Phys.* 19, 3 (1996)

[3] S. W. McDonald, *Phys. Rev. A* 43, 4484 (1991)

[4] H. Weber *et al.*, *EPJ Web of Conf.* 87, 01002 (2015)

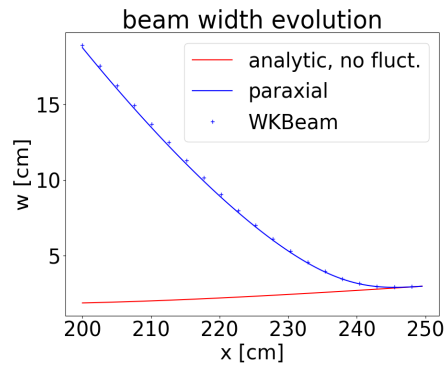


Fig.1: Example of propagation in free space plus fluctuations as a simple test case: For a relatively large correlation length of the density fluctuations WKBBeam and paraxial expansion of the WKE are in good agreement. The analytical reference does not include the effect of fluctuations.

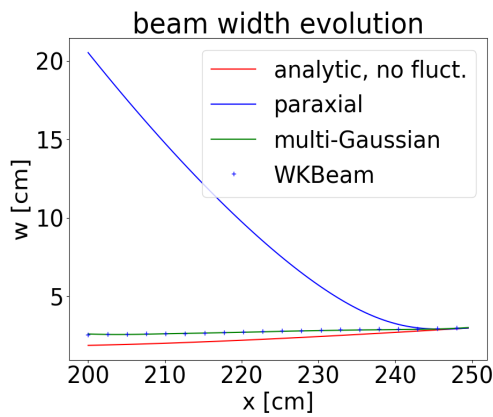


Fig.2: Same as Fig. 1 but with a shorter correlation length: in this case, the paraxial expansion of the WKE cannot reproduce the result of WKBBeam. However, the multi-Gaussian approach solved in terms of a Monte-Carlo scheme does.

# Modeling Coulomb Interaction with a 'Wigner-Poisson' Coupling Scheme

Mauro Ballicchia<sup>1</sup>, Majid Benam<sup>1</sup>, Mihail Nedjalkov<sup>1</sup>,  
Siegfried Selberherr<sup>1</sup>, and Josef Weinbub<sup>2</sup>

<sup>1</sup>*Institute for Microelectronics, TU Wien, Austria*

<sup>2</sup>*Christian Doppler Laboratory for High Performance TCAD,  
Institute for Microelectronics, TU Wien, Austria  
josef.weinbub@tuwien.ac.at*

Entangled quantum particles, for which operating on one particle instantaneously influences the state of the associated particle, are attractive for carrying quantum information at the nanoscale. However, describing entanglement in traditional time-dependent quantum transport simulations requires doubling the degrees of freedom, involving an almost prohibitive computational effort. Considering electrons, one approach to analyze their entanglement is through modeling the Coulomb interaction (Coulomb Entangler) via the Wigner formalism. We showed that the computational complexity of the time evolution of two interacting electrons is reduced by approximating the Wigner equation in the two-particle phase space by two equations, each defined in a single-particle phase space [1]. In particular, we replace the non-local Wigner potential operator of the electron-electron interaction by an electrostatic field which is introduced through the spectral decomposition of the potential. The coupling between the two equations, based on a consecutive update of the electric field, establishes the entanglement. It is demonstrated that for some particular configurations of an electron-electron system, the introduced approximations are feasible. Purity, identified as the maximal coherence for a quantum state, is analyzed and it is consequently demonstrated that entanglement due to Coulomb interaction is well-accounted for by the introduced local approximation. Fig.1(a) shows the purity of two electrons without Coulomb interaction. The first electron is injected into the simulation region within 60 fs. After the complete injection of the electron the uncertainty rule is satisfied and the purity stabilizes at the perfect value one, which prevails, until the electron starts to exit the simulation region after about 190 fs. The injection of the second electron begins 70 fs after the first one, indicated by the blue curve. In the time interval between  $t = 140$  fs and  $t = 190$  fs, highlighted by the dashed red lines, both electrons evolve quantum mechanically, without interaction as two independent pure states. Fig.1(b) focuses on this time interval and shows the purity being perfectly equal to one. Fig.2(a) demonstrates the effect of Coulomb repulsion. To better highlight the influence, the charge of each electron is increased by an order of magnitude. Accordingly, at  $t = 140$  fs the purity starts to drop at the beginning of the interaction. The level of entanglement due to the Coulomb interaction increases during the evolution, which is well-demonstrated by the continuous decline of the purity. As can be seen in Fig.2(b), the purity evolves equally for both electrons as expected.

[1] M. Benam *et al.*, J. Comput. Electron. 20, 775-784 (2021)

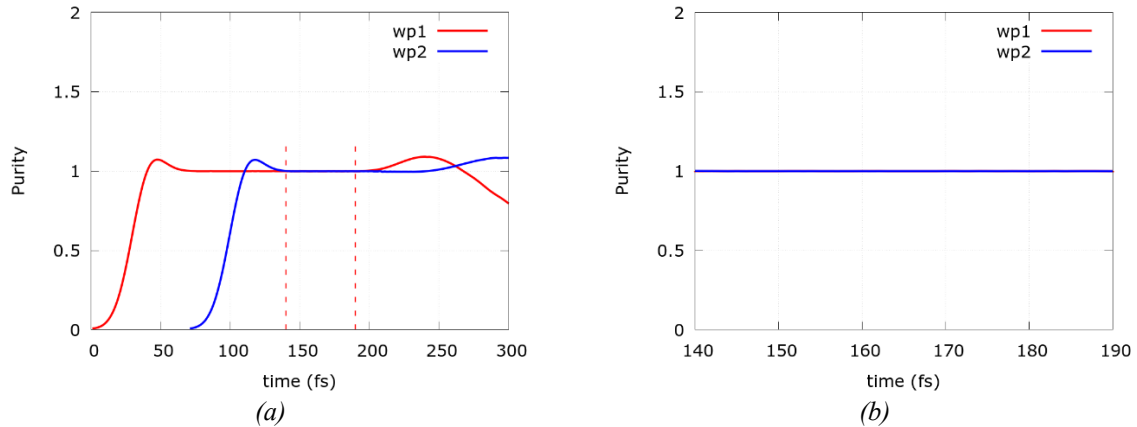


Fig.1: Time evolution of the purity of two non-interacting wavepackets (wp), i.e., electrons, for (a) the entire evolution time (dashed red lines indicate time interval shown in (b)), and (b) the time interval from  $t = 140$  fs to  $t = 190$  fs. Reprinted with permission from [1]. Copyright 2021 Author(s), licensed under Creative Commons Attribution 4.0 International.

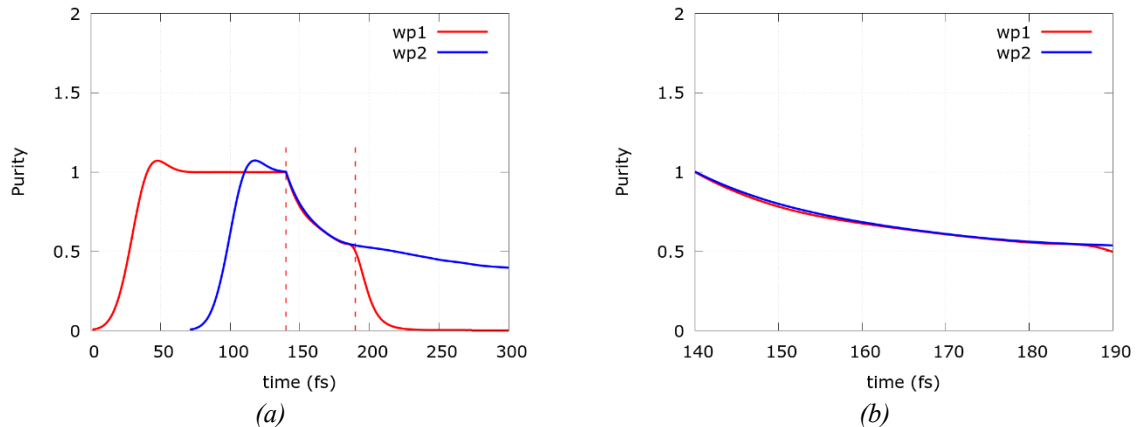


Fig.2: Time evolution of the purity of the two states in the Coulomb Entangler for (a) the entire evolution time (dashed red lines indicate time interval shown in (b)), and (b) the time interval from  $t = 140$  fs to  $t = 190$  fs. Reprinted with permission from [1]. Copyright 2021 Author(s), licensed under Creative Commons Attribution 4.0 International.

**Acknowledgements.** The financial support by the Austrian Science Fund (FWF): P29406 and P33609, the Austrian Federal Ministry for Digital and Economic Affairs, and the National Foundation for Research, Technology and Development is gratefully acknowledged. The computational results presented have been achieved using the Vienna Scientific Cluster (VSC).

ISBN 978-3-9504738-2-7



9 783950 473827 >